Growth Mechanism of Carbon Nanotubes Revealed by *in situ* Transmission Electron Microscopy

Lili Zhang[1], Dai-Ming Tang[2,3], Chang Liu[1,*]

[1] *Shenyang National Laboratory for Materials Science, Institute of Metal Research, Chinese Academy of Sciences, 72 Wenhua Road, Shenyang 110016, China,*
[2] *Research Center for Materials Nanoarchitectonics (MANA), National Institute for Materials Science (NIMS), Tsukuba, 305-0044, Japan*
[3] *Department of Materials Science, Faculty of Pure and Applied Sciences, University of Tsukuba, Tsukuba 305-8573, Japan*

Corresponding author(s): cliu@imr.ac.cn

Abstract

Elucidating the growth mechanism of carbon nanotubes (CNTs) is critical to obtaining CNTs with desired structures and tailored properties for their practical applications. With atomic resolution imaging, *in situ* transmission electron microscopy (TEM) has been a key technique to reveal the microstructure and dynamics of CNTs in real time. In this review, recent advances in the development of *in situ* TEM with different types of environmental reactors will be introduced. The catalytic growth mechanisms of CNTs revealed by *in situ* TEM under realistic conditions are discussed from fundamental thermodynamics and kinetics to the detailed nucleation, growth, and termination mechanisms, including the state and phase of active catalysts, interfacial connections between catalyst and growing CNTs, and catalyst-related growth kinetics of CNTs. Great progresses have been made on how a CNT nucleates, grows and terminates, focusing on the interface dynamics and kinetic fluctuations. Finally, challenges and future directions for understanding the atomic dynamics under the real growth conditions are proposed. It is expected that breakthroughs in the fundamental growth mechanisms will pave the way to the ultimate goal of designing and controlling the atomic structures of CNTs for their applications in various devices.

1. Introduction

In the past three decades, carbon nanotubes (CNTs) have gained substantial attentions among researchers and industries due to their unique one-dimensional tubular structures

and excellent physicochemical properties.[1, 2] They are considered ideal candidates as ballistic conductors in transistors[3], super-strong fiber materials,[4] and structural models leading the science and forefront of nanotechnology.[5] However, there is still a great challenge to control the atomic structure, such as diameter and chirality of CNTs, which ultimately determines their performance in functional devices such as transistors.[6]

With the aim to obtaining CNTs with uniform structures and properties, notable developments have been achieved recently in controlling the growth of single-wall CNTs (SWCNTs) with specific chirality, by catalyst designing and kinetic modulation in chemical vapor deposition (CVD).[7, 8] However, the growth mechanism remains largely a "black box", because CNT growth is a small-scale and complex process, involving multi-phase reactions, phase transition and mass transport at elevated temperature and gaseous environment. The term 'growth mechanism' here and in the title refers generically to the mechanisms of CNT formation, from cap formation and lift-off, tube elongation and cessation, etc. Whereas, 'growth mechanism' in section 3.3 refers specifically to the elongation mechanism of CNT sidewall, which is a process between CNT nucleation and growth termination. Over the past decades,ten major open questions on SWCNT growth mechanism have been summarized,[9] and both experimental and theoretical studies have been performed to reveal why and how a CNT can grow, and how it grows in a controlled way.[10, 11] Despite tremendous previous efforts, the critical roles of catalyst and other growth parameters on the dynamic formation processes of CNTs remain contradictory, due to the lack of direct evidence regarding the catalyst state, catalyst-tube interface and growth kinetics.

Transmission electron microscopy (TEM) is capable of characterizing microstructures and compositions of nanomaterials at the atomic level and has long been applied in CNT research as reviewed in Section 2.1. *In situ* TEM especially environmental TEM is a powerful tool for visualizing both atomic structures and their dynamical evolutions of nanomaterials under reactive environments in real time. Compared to traditional post-growth characterization methods, *In situ* TEM plays a substantial role in revealing the synthesis mechanism of nanomaterials,[12, 13, 14] from which high spatial and temporal information can be obtained by observing the reaction kinetics. With the supplies of gaseous environment and controlled temperature from e-beam effects, electrical stimulus or heating by a chip (Section 2.2), *in situ* TEM can

mimic CVD growth of CNTs from catalysts and record multi-phase reactions involving growth parameters, catalyst, CNT or support, providing valuable opportunities to address the fundamental questions by tracking structural dynamics of these nanomaterials in each reaction stage.

There have been many excellent reviews on the topic of CNTs growth mechanism,[15] from growth dynamics,[16] structure-controlled growth,[17, 18] to theoretical simulation.[19] in situ environmental TEM has been reviewed comprehensively, with topics ranging from development of ETEM[20], and applications in heterogeneous catalysis, including gas phase catalyst and synthesis.[14, 21, 22] Our review provides updated, focused and in-depth technical progress and mechanistic understanding on the fundamental mechanisms of CNTs growth by in situ TEM. Various in situ reactors are introduced and compared regarding the configuration, pressure and imaging resolution for observing CNTs growth inside a TEM. Then, growth mechanisms of CNTs are comprehensively discussed based on direct observations from in situ TEM. Structures and key roles of catalysts on CNT growth thermodynamics and kinetics under realistic conditions are highlighted, and the details on CNT nucleation, growth and termination processes are discussed. Finally, the developing trend of in situ environmental TEM (ETEM) to tackle the challenges in understanding the growth mechanisms of SWCNTs and ultimately to precisely controlling their atomic structure and properties will be proposed. a perspective is provided for the CNTs growth mechanism research from atomic structures to atomic dynamics, based on applications of advanced electron microscopy.

2. Progress on the Study of CNT Growth by *in situ* TEM

2.1 Application of TEM in CNT Research

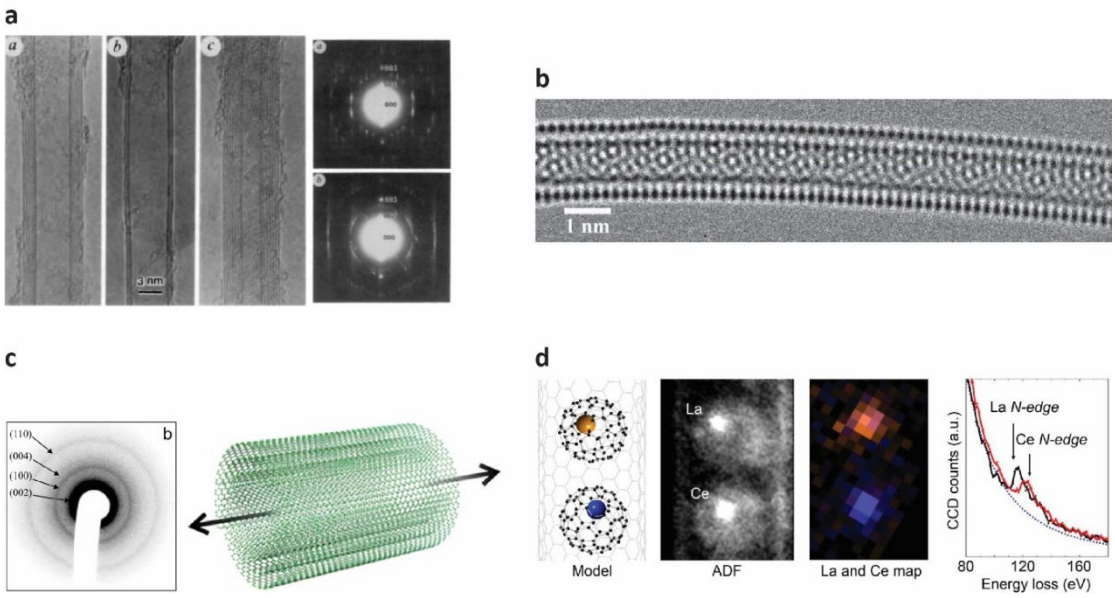

Figure 1. Application of TEM in CNT research. (a) Discovery of CNTs by TEM observation and helical structures revealed by ED.[1] (b) Atomically-resolved CNT structure by aberration-corrected TEM.[23] (c) Lattice vibration revealed by ultra-fast TEM and ED.[24] (d) Chemical analysis of individual atoms confined within carbon peapods.[25]

TEM had been a key instrument in the discovery of CNTs, showing their one-dimensional tubular structure with small diameters in nanoscale (Figure 1a).[1] In addition, TEM was indispensable to investigate the fine structures of CNTs, including the unique chiral structures that were resolved by electron diffraction (ED). As we will discuss in Section 3, *in situ* environmental TEM is a crucial technique that can reveal both the atomic structure and growth dynamics of CNTs in real time.

Historically, the resolution of TEM is limited by the aberration of electromagnetic lens. The revolutionary invention of aberration correctors[26] made it possible to resolve the atomic structures with sub-Angstrom resolution at a relatively low accelerating voltage (60 kV or even lower). Therefore, detailed atomic structures of CNTs could be resolved, including strain in CNT lattice,[27] topological defects in SWCNTs,[28] and atomic defects of the inner-wall in a double-wall CNT (Figure 1b).[23] Associated with the observation in real space by TEM imaging, ED is a complementary method to analyze the crystalline structure in reciprocal space. In 1991, Iijima identified the

helical structure of CNTs by analyzing the unique ED patterns[1] which showed similar features as that from the helical structures of DNA. In contrast to the complex features in TEM images of CNTs due to the wrapping and overlap of upper and lower walls, clear layered lines in EDs could be used to analyze the chirality of CNTs simply and precisely.[29] Zewail group developed ultrafast TEM and ED with sub-picosecond and sub-picometer resolutions, and revealed the lattice dynamics in CNTs (Figure 1c).[24]

In addition to the parallel illumination in TEM and ED modes, by focusing the electron beam into a small probe, it can be used to image the microstructure in a scanning manner and to analyze the local structure, combining with spectrometers such as energy dispersive X-ray spectroscopy (EDS) and electron energy-loss spectroscopy (EELS). With the help of probe correctors, it has been routine for the modern STEMs to have a resolution in the sub- Ångström region. Typically, an annular dark field (ADF) detector is used to collect incoherently scattered electrons, and in the meantime an EELS spectrometer is used to get the information from inelastically scattered electrons. Because of the so-called Z contrast that is proportional to $Z^{1.7}$, where Z is the atomic number of the elements, single-atom sensitivity has been demonstrated for the metal atoms anchored on graphene surface or "peapods" of fullerene confined in nanotubes (Figure 1d).[25, 30]

In recent years, the energy resolution for STEM-EELS has been dramatically enhanced to ~10 meV level, therefore, not only the composition information from the energy loss of inner shell electrons,[31] but also information from the low-loss region could be obtained to understand the electronic, optical[32] and even phononic[33] structures of individual low dimensional materials. For example, the temperature distribution of Joule-heated individual CNTs could be mapped by analyzing the shift of the plasmon peaks.[34]

STEM has not been widely used for the characterization of CNTs, due to the small Z number of carbon element and their complex geometry. Essentially, CNTs belong to the group of "weak-phase-objects", which changes the phase but barely the amplitude of electron waves during scattering, leading to a low contrast and small signal-to-noise ratio in ADF-STEM images. Normally, only the amplitude of the electrons could be recorded by the detectors and the phase information is lost. That is the "phase problem". There are several ways to reconstruct the phase and to resolve the microstructures of the weak-phase-objects. One method is STEM-Ptychography, where the convergent

beam ED patterns during the scanning are recorded to a 4D database. Ultra-high resolution of ~0.2 Å has been demonstrated, where the limit is thermal vibrations of the atoms.[35] Since the contrast of STEM-Ptychography is linearly proportional to the atomic number, both light and heavy atoms could be resolved. Three dimensional complex crystalline structures confined in double-wall CNTs were revolved by applying the ptychographic atomic electron tomography.[36]

2.2 *In situ* TEM Reactors for CNT Growth

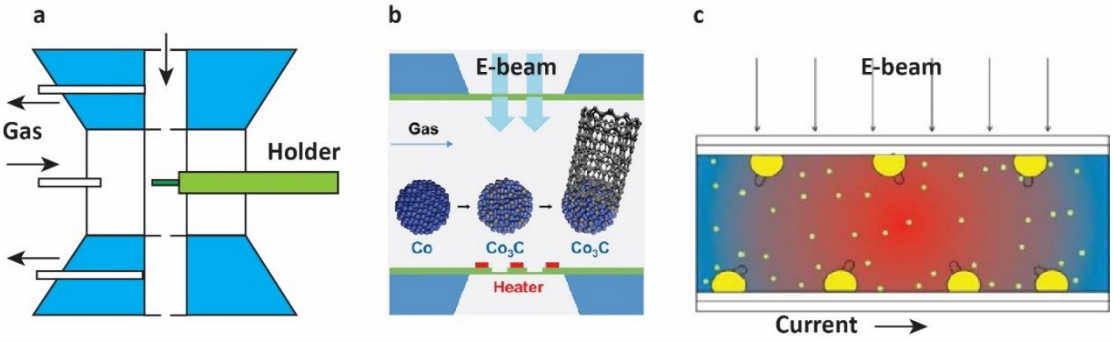

Figure 2. *In situ* TEM reactors for CNT growth. (a) Milli-reactors based on ETEM. (b) Micro-reactors based on close-cells.[37] (c) Nano-reactors based on CNTs.[38]

By introducing various stimuli into TEM, *in situ* TEM techniques have been developed to not only characterize the atomic structures but also to investigate the atomic dynamics, and to associate them with the processing conditions and physical properties. There have been many excellent reviews on the topics of *in situ* TEM probing and gas-phase ETEM.[22, 39] Here we focus on *in situ* TEM reactors for investigating the growth mechanisms of CNTs, including milli-reactors based on ETEM, micro-reactors based on closed-cells and nano-reactors based on individual CNTs.

To grow CNTs inside a TEM chamber, one essential challenge is to fulfill the "growth conditions" while keeping a "high resolution" of the TEM. To realize the CNT growth, there should be a carbon source, either in gas phase or in solid phase, catalyst, and temperature up to around 1000 ºC. To investigate the growth mechanism, the reactor needs to be transparent enough so that the electron beam could be transmitted and kept a small enough beam broadening to get a high-resolution image. Normally, there is a compromise to solve the conflict. And that is why there is no perfect solution, but rather a variety of complementary approaches.

2.2.1 ETEM: Milli Reactors

The design of ETEM is to create a local gas environment near the specimen while keeping other part of the TEM column in high vacuum (Figure 2a).[40] Smaller apertures combined with additional pumps are used to realize the differential pressure. Therefore, ETEM is also called as differential pumping environmental cell, or open-cell ETEM. ETEM is compatible with different kinds of TEM holders, since it is the TEM chamber modified to create gas environments. Furnace type heating holder have been used in the early times, where it took minutes to change the temperature and the images suffered from thermal drifting. Nowadays, MEMS-based heating holders are typically used in ETEMs so that the temperature could be adjusted with a heating rate as high as 1000 K/s. Because of the low density of gas, about 1000 times smaller than that of solids, the scattering and broadening of electron beam is minimized so that atomically resolved TEM and STEM images can be obtained for the catalysts. However, the resolution will be limited by the scattering from gases, due to the millimeter scale pole piece gap, if the gas pressure is increased. Therefore, the maximum pressure for ETEM is typically limited to about 2000 Pa.

As early as in the 1970s, Baker *et al.* have applied ETEM to study the growth process of carbon nanofibers.[41] And in 2004, both multi-wall CNTs and SWCNTs were grown by using ETEM.[42] Since then, great progress has been made to reveal the growth mechanisms of CNTs, from the physical state and phase structure transition metal catalysts[43-45, 46, 47] to the nucleation of carbon caps and transformation from graphene to nanotubes.[48] However, because the reactor is open and the size of the reactor is small (a few millimeters), the upper limit for the gas pressure is much lower than the typical gas pressure for growing CNTs by CVD (10^5 Pa). Thereby, atmospheric-pressure TEM is required to fill the pressure gap.

2.2.2 E-Cell: Micro Reactors

E-Cells, the so-called “close-cell” ETEM, have been designed to fill the pressure gap of ETEM (Figure 2b). Membranes made of silicon nitride (SiN_x) thin films are used to seal gas in a micro-reactor that is fabricated by using MEMS technology.[49] Because of the high mechanical strength[50] and chemical inertness, E-Cells with SiN_x membrane windows could be used for various chemical conditions, such as oxidative and reductive atmospheres, and the pressure could be as high as 4×10^5 Pa.[51] In addition, since the thickness of a single SiN_x membrane is around 20-50 nm, they still can be transmitted

by electron beams with a high accelerating voltage. By using ADF-STEM imaging, individual atoms, detailed surface structures of the catalysts during chemical reactions could be clearly resolved.[52] In combination with the membrane, micro-heaters are fabricated so that the local temperature close to the observation windows could be increased with a high speed and a high stability.[53]

Compared with dedicated ETEM, which requires modifications to the TEM chamber, E-Cells are compatible with most commercial TEMs. Therefore, there are more groups working on the E-Cell approaches nowadays. And the growth mechanism of CNTs under atmospheric pressure had been investigated. Most of the publications are focused on the state and dynamics of catalysts, including transitional metals such as Fe,[54] Ni,[55] Co,[37] Ru,[56] and alloys including Ni-Co[57] and Co-W catalysts.[58] It is worth noting that at atmospheric pressure, carbide phases were observed to be the active phases for Fe, Ni and Co. In contrast, at a low pressure in ETEM, it was reported that Co catalyst has a mixed phase of Co-Co_2C[47] and Ni catalyst typically keeps its metallic phase.[43]

A limitation and great challenge for E-Cells is from the interaction between electron beam and the SiN_x membrane windows. Especially for CNTs, because of the small atomic number, which is smaller than those of Si and N, the contrast and resolution for CNT images is greatly reduced. Therefore, it is challenging to investigate the detailed growth mechanisms such the interfacial structural dependence between the catalysts and CNTs.

2.2.3 CNT-Cell: Nano Reactors

In addition to ETEM and E-Cell (close-cell ETEM), there is another special approach to investigate the chemical reactions and growth mechanisms of nanomaterials. That is the nano-reactors based on individual CNTs (Figure 2c). CNTs are mechanically strong and electrically conductive, therefore, a CNT could be heated by Joule heating or electron beam irradiation to a high temperature. Instead of a gaseous carbon precursor, by utilizing the elastic scattering of electron beam and the wall of the CNT, carbon atoms could be injected into the catalysts confined within the hollow channel,[59] so that the interaction of carbon and the catalyst and the nucleation-growth process of CNTs could be investigated at atomic resolution.[38, 60, 61] Note that with a MEMS-based heating holder, carbon nanofibers[62] or carbon films can also be used as solid carbon precursors and support like CNTs for *in situ* TEM studies.

Chuvilin *et al.* observed the coalescence of fullerenes and final formation of an inner

wall in a SWCNT, where individual dysprosium atoms played a key role to catalyze the process.[63] Zoberbier *et al.* demonstrated that both the lattices of the nanotube reactor and metal clusters could be revealed by low-voltage aberration-corrected high-resolution TEM,[64] to investigate the bonding behaviors of various transition metals with carbon. Comparative studies on the catalytic behavior of traditional iron oxide and gold catalysts revealed the reaction path from Fe_2O_3 to Fe_3C for the nucleation and growth of CNTs, while fluctuations in shape, size, and orientation were observed for Au nanoparticles.[38]

2.2.4 A Comparison of *in situ* TEM Reactors

Table 1 Comparison of in situ TEM reactors for CNTs growth mechanism

	DP-ETEM	E-Cell	NT-Cell
Size	millimeter	micrometer	nanometer
Pressure (Pa)	2000	400000	1.E-04
Carbon source	Gas	Gas	Solid
Heating	Furnace, MEMS	MEMS	Joule heating
Maximum temperature (K)	1273	1273	2000
Resolution (nm)	0.2	0.3	0.1
Applications	Low-pressure growth	Atmospheric-pressure growth	Solid state reaction
Limiting factor	Gas pressure	Membrane scattering	Solid state carbon source

We have compared the three types of in situ reactors for investigating CNTs growth mechanism in Table 1, regarding the size, pressure, temperature, resolution, typical applications and limiting factors. Xin *et al.* conducted simulations of TEM images of ETEM and E-Cell, by considering the broadening effects from elastic scattering and chromatic aberrations from inelastic scattering.[65] The elastic broadening follows a $t^{3/2}$ power law with the sample thickness (t), and the chromatic blurring scales linearly with thickness. It was predicted that while near Ångström resolution could be obtained for aberration-corrected ETEM, the optimum resolution for E-Cells with a SiN_x thickness of 37 nm was ~0.38 nm, which is not enough to resolve most of the crystalline lattices. However, for the heavy metals, the Pd/Pt (111) lattice planes with interplanar distances of 2.2 Å were resolved under gas flow and heating conditions, due to the strong

diffraction conditions and nonlinear effects.

Koo *et al.* studied the influence of membranes to the STEM images by simulations on BiCuSO crystals in a E-Cell with the SiN_x thickness to be 50 nm.[66] For STEM images in bright field (BF) and annular bright field (ABF) modes, the signal contrast was very low (~0.04) close to a noise level. For ADF-STEM images, compared with a vacuum background, the noise level was increased for 100 times for ETEM, and 1000 times for E-Cells. Still, the contrast (~2.5) for ADF-STEM is much higher than those of STEM images in ABF and BF modes. As a result, for the heavy metal atoms, it is possible to resolve the atomic structures clearly.

The above discussions and simulations indicate that the open reactor is the limiting factor for the low gas pressure in ETEM, and the SiN_x thickness of E-Cells is the limiting factor for the imaging resolution. We have carried out TEM simulations of metal nanoparticle attached to the ends of CNTs.[58] While the lattices of metal particles can be resolved even with the SiN_x thickness to be 30 nm, lattices of CNTs could not be clearly seen with the SiN thickness larger than 5 nm. In the future, it would be desirable to design and fabricate E-Cells with the membrane thickness smaller than 5 nm. Two-dimensional materials such h-BN are suitable candidates for the membranes, because of its high mechanical strength and chemical inertness.

3. Progress on the CNT Growth Mechanisms by *in situ* TEM

In situ TEM is a powerful tool for tracking the growth processes of CNTs at high temperatures and under carbon-containing gaseous conditions, as well as investigating the influence of growth parameters and catalyst nanoparticles on the structure of grown CNTs (Figure 3a). Based on the recent advances of *in situ* TEM techniques, the catalyst activity, selectivity and stability, as well as relationships between catalysts and CNTs, catalysts and supports, conditions-dependent CNT growth kinetics are presented from the viewpoint of CNT growth thermodynamics and kinetics (Section 3.1). Compared to post-growth (*ex situ*) TEM characterization, *in situ* ETEM with advanced aberration correctors allows for the resolution of atomic-scale structures of catalysts during CNT growth. Especially, *in situ* E-cell TEM studies of catalytic growth of CNTs bridges pressure gap between ultrahigh vacuum for traditional characterizations and atmospheric-pressure for complex CVD growth conditions. Despite the more complex catalyst systems and gaseous environments involved, researchers have taken a significant step in unveiling how a CNT nucleates and grows from active catalyst

nanoparticles, as well as CNT growth kinetics with catalyst evolutions (Sections 3.2-3.3). We finally present recent progresses on the termination of CNT growth in Section 3.4.

3.1 The Thermodynamics and Kinetics of CNT Growth

It is well-known that thermodynamics and kinetics are the two fundamental perspectives to understand how a material nucleates and grows in a controllable way. Recently, it has been demonstrated that both the catalyst features as the main thermodynamic factors and the growth conditions as kinetic effect contribute to the chirality-specific growth of SWCNTs.[67] Therefore, it is necessary to clarify their roles during CNT growth.

CNT growth involves several basic processes like carbon dissociation, adsorption, diffusion and precipitation through catalysts. The multi-phase interactions between temperature, gaseous environment, catalyst (or together with support) and grown CNT are vital for understanding the process. This section will firstly introduce the identification of the state, morphology and phase of catalyst, catalyst-CNT and catalyst-support interfacial interactions during CNT growth by describing catalyst activity, selectivity and stability. Then, factors such as temperature, pressure and carbon feeding concentration determining CNT growth kinetics will be discussed. It is important to note that the catalyst structure and its evolution during CNT growth can be observed in real-time on the atomic-scale by *in situ* TEM,[13] showing advantages in understanding catalytic reaction mechanism than other approaches such as environmental SEM[68] and environmental optical microscopes or spectroscopes.[10] In addition to playing key roles in the thermodynamics of CNT growth, catalyst also has an impact on the kinetics of CNT growth, which will be discussed in Section 3.3.

3.1.1 Determining the State, Morphology and Phase of Catalyst

The chemical and physical states of catalyst nanoparticles may affect the growth thermodynamics and kinetics of CNTs and ultimately determine their structures. Thus, determining active phase, morphology and physical state of catalysts under reaction conditions is essential in elucidating the activity, selectivity and stability of catalysts during CNT growth, which will be described as follows.

It has been well believed that not all prepared catalyst particles are active in growing CNTs, Chao *et al.* reported that there is a catalyst structure and activity relationship for

CNT growth observed under ETEM.[69, 70] Especially, catalysts can undergo a phase transition prior to or during CNT growth, it is therefore necessary to *in situ* investigate the dynamic behaviors of active catalyst nanoparticles in reactive environment. Taking the mostly used transition metal catalyst Fe as an example, the active phase of Fe catalyst nanoparticles for CNT growth was revealed as Fe_3C[44, 71] during CNT growth and the inactive phase was Fe_2C_5, which was attributed to their difference in surface activity for C diffusion and C-C bond formation.[71] However, the active Fe phases were demonstrated differently depending on original phase compositions of catalyst particles for CNT growth by *in situ* grazing-incidence X-ray diffraction. For austenite Fe, metallic Fe is the active phase, while carbide is the active one for ferrite Fe.[46] These collective results indicate that the assumption of a single active catalyst phase is not valid, the actual nature of active catalysts is related to the realistic CNT growth recipes and there might be kinetic effects dominate catalyst phase evolution.

Co catalyst is a typical example whose active phase structure is often controversial, it was summarized that Co, Co_3C, Co_2C and mixed phases have all been previously reported by either *ex situ* or *in situ* TEM.[37] The Co_2C or Co_3C phase in some cases favors the nucleation and growth of SWCNTs, while in some other cases, the Co_3C phase is inactive or fluctuates between Co_2C and Co to grow SWCNTs. Such inconsistency in the active phase structures of a Co catalyst not only comes from different CNT growth recipes, but also the similarity of the diffraction patterns of hcp Co, orthorhombic Co_2C and orthorhombic Co_3C phases. It is therefore necessary to distinguish the phases not only from one particle or one diffractogram. In order to precisely determine the active phase of catalysts for a better understanding of CNT growth mechanisms, we performed direct growth of CNTs from Co catalyst at near-atmospheric pressure using an E-cell ETEM, and developed a strategy based on a large amount of *in situ* TEM data, statistical analysis of the electron diffractograms with strict error criteria. The active phase was precisely identified as orthorhombic Co_3C phase and remains unchanged during CNT growth despite dynamic changes in their morphology and orientation (Figure 3b).[37]

Theoretical calculations were also performed to verify the relative stability of Co_3C phase under CNT growth conditions. It is confirmed that with a relative higher carbon chemical potential and higher temperature (around 1000 K), Co_3C becomes the most stable phase, while the active phase structure can change to Co_2C or Co as function of

temperature, particle size and relative chemical potentials of carbon[37] (Figure 3c), e.g., catalysts might be in the Co_2C phase for smaller SWCNTs at a lower temperature. For a SWCNT growth from a sub-2 nm Co particle at a lower pressure of carbon source and a lower temperature under ETEM, Sharma group identified Co and Co_2C as active phases for Co catalysts and their distinct regions were observed to fluctuate during SWCNT growth.[72] All of the assignment of phases and evolution information would provide solid basis to evaluate the stability or behaviors of catalyst particles and carbon cycle kinetics through catalyst as well as the growing CNTs,[58, 72] For instance, there are two possible routes for carbon supply during multi-wall CNT growth (Figure 3d), while the surface and interface diffusion instead of the previous bulk diffusion support the fast growth of CNTs from the solid Co_3C catalyst.[37]

Previously, the active phase of Ni catalysts has been well-recognized as metallic Ni by carbon surface diffusion under low-pressure ETEM[43, 73, 74]. While recently, Liu et al. have drawn a conclusion by using *in situ* ETEM that Ni_3C is the working catalyst phase for CNT or nanofiber growth by a bulk diffusion path of carbon atoms.[75] With the above precise identification method, we have also characterized the atomic structures of Ni during CNT growth under atmospheric-pressure E-cell, both metastable Ni and Ni_3C were identified to be active phases, allowing for correlating the catalyst phase structure and morphology with carbon cycle kinetics through the growing CNTs.[76]

High-melting point alloy catalysts such as Co-W nanoparticles have been reported to be effective for the structure-controlled growth of SWCNTs. Several groups have attempted to clarify the intriguing issue of their actual phase structures and behaviors of the catalysts during CNT growth. Based on ETEM studies, Yang *et al*.[77] identified the catalyst nanoparticles as intermetallic phase of Co_7W_6, which was demonstrated stable at high temperature even with carbon feeding. Differently, An *et al.*[78] identified the sputtered Co-W-C catalyst to be a junction of the W-enriched phase and Co_6W_6C, but it evolved into a mixture of Co_6W_6C and Co or Co-enriched phases upon the introduction of carbon source. Because of the post-growth characterization using atomic-resolution scanning TEM, the active phase for CNT growth is still unclear. By realizing the *in situ* E-cell growth of CNTs at atmospheric pressure, we characterized the atomic structures of the sputtered catalyst particles and the growing CNTs simultaneously under the growth condition, the active phase was determined to be a

stable single phase of cubic Co-W-C ternary carbide (Figure 3d).[58]

The precise identification of active phase of catalyst nanoparticles shall play critical roles in determining CNT growth thermodynamics and structures. For example, we found that a SWCNT can grow from a single phase of Co-W-C alloy particle tangentially, so that the tube diameter can be determined directly by the particle size. In the other two cases,[77, 78] a smaller SWCNT was believed to grow from a much larger particle, either a certain facet of the Co_7W_6 phase or Co_6W_6C phase was attributed to nucleate SWCNT, while because of the evolution of Co_6W_6C phase, the precipitated Co phase might also contribute to the diameter or chirality-selective growth of SWCNTs. In addition, Chiang *et al.* has demonstrated that SWCNT chirality distribution can be altered by varying the Ni_xFe_{1-x} catalyst compositions, which can introduce perturbations to the crystal structures and then influence the epitaxial lattice match with certain chiralities.[79] However, there is an indirect link between the chirality distribution and catalyst structure, it is still expected to systematically investigate the interfacial interactions directly between phase composition of catalysts and the resulting SWCNT chirality.

We have also demonstrated that the CNT growth rate from this alloy catalysts is two orders of magnitude slower than the that from Co_3C catalyst, because both kinds of catalysts prefer to follow surface and interface diffusion of carbon atoms for CNT growth rather than bulk diffusion, and the activation energies for both surface and interface diffusion on Co_3W_3C are larger than that for solid Co_3C, as confirmed by theoretical calculations (Figure 3e). We therefore conclude that catalyst phase structure or composition can strongly influence the growth kinetics of CNTs, shedding light on design of catalysts for the chirality control of SWCNTs.

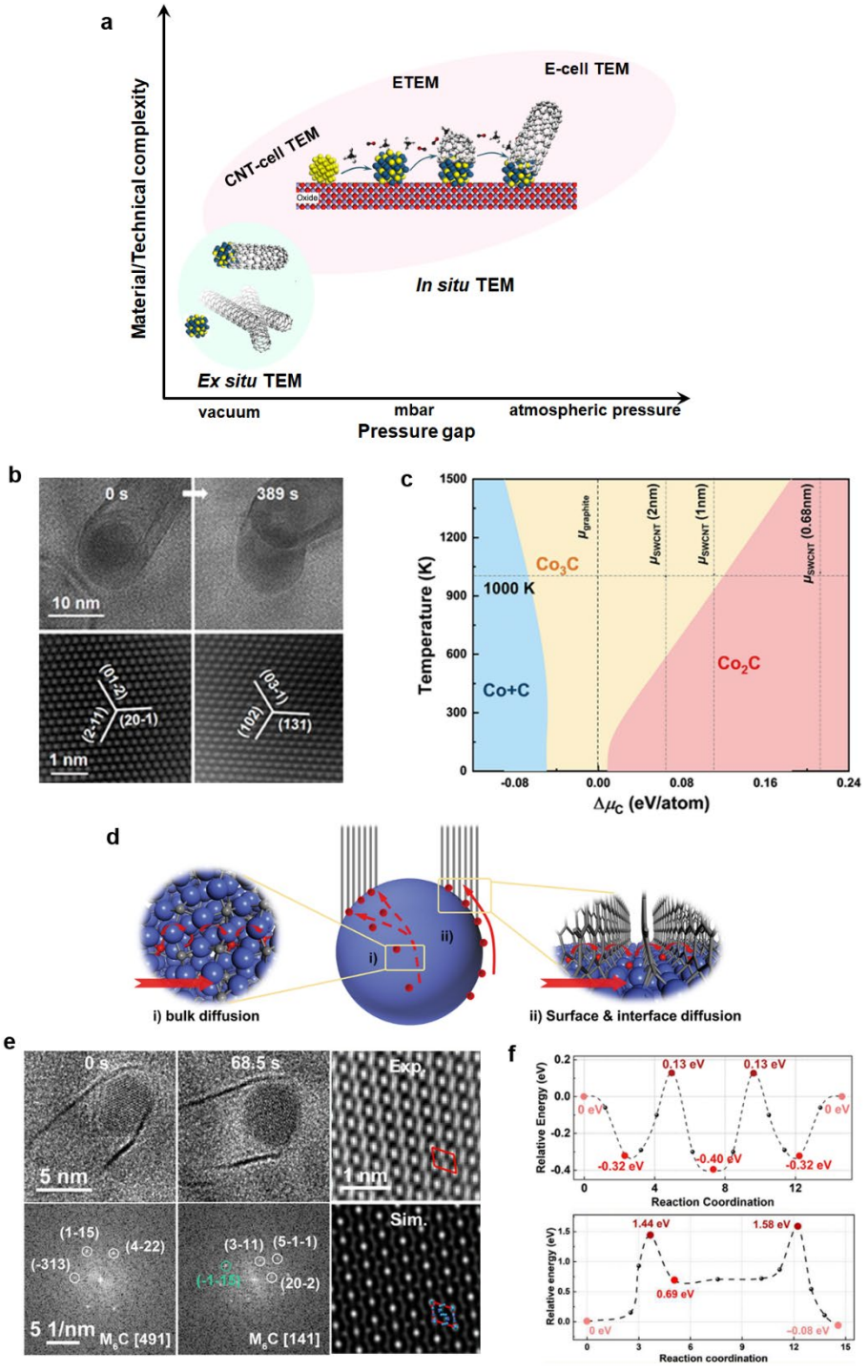

Figure 3. (a) *Ex situ* and *in situ* TEM studies of catalytic growth of CNTs showing the pressure gap and technical/material complexity. By bridging pressure gap with *in situ* E-cell TEM, catalyst phases can be identified during CNT growth under real reactive conditions. (b-d) Identifying the active phase of a Co catalyst during CNT growth under E-cell TEM, and the theoretical calculations on the phase stability and carbon diffusion path.[37] (d) Phase identification of Co-W-C catalysts connecting to the

growing CNT at atmospheric pressure. (e) The minimum energy path for carbon atoms along the interface diffusion process between a CNT and Co_3C catalyst (top) or Co_3W_3C catalyst (down).

Catalyst selectivity is another crucial issue in the preferential growth of CNTs, which mainly involves the features of catalysts under reaction conditions. Despite the above active phase structures, morphology, shape, symmetry of catalysts are also important in selectively growing SWCNTs with specific structures (chirality, diameter, etc.) and properties.[7] However, linking the morphology and structures of catalyst to the preferential growth of CNTs is still limited by the difficulty in preparing nanoparticles with suitable sizes and specific morphologies, and characterizing CNT structures under growth conditions. So far only evidence of gas-catalyst interaction was provided by *in situ* TEM, the preferential growth issue was then discussed in conjunction with CVD growth results. Harutyunyan *et al.*[80] demonstrated that the annealing behaviors Fe catalysts changed by varying noble gas environments under ETEM. In the presence of He/H_2O, the particle can be coarsened and faceted, while Ar/H_2O annealing ambient leads to a round morphology. These catalyst rearrangements or dynamical alternations in the particle shape were attributed to the changes of surface energy anisotropy of specific facets, and indirectly correlated to the preferential growth of CNTs by CVD.

Although the understanding is not in the context of the complex catalyst-tube relationship such as nucleation processes of CNTs, the design and synthesis of faceted solid catalysts with specific morphology became an insightful direction for the controlled growth of CNTs. The synthesis of a faceted Pt catalyst particle with a suitable size for CNT growth has been recently explored under atmospheric pressure,[81] suggesting that investigation on the template effect of catalysts on selectivity of SWCNTs could be possible.

Catalyst stability under realistic conditions is mainly influenced by (1) melting point and carbon solubility, (2) substrate effects and (3) carbon adsorptions on catalyst surface. The melting points of different metal catalysts and carbon solubility are the criteria for the physical state of catalysts during elevated temperature, i.e., high thermal stability. Catalyst with low melting points and high carbon solubility, such as Fe, Ni catalyst particles, were found to be in the liquid-like state under realistic CNT growth conditions,[43, 44, 73] the mechanism is termed as the vapor-liquid-solid (VLS).[82] Catalysts with high melting points such as diamond, alloy, oxide and carbide are

believed in solid state during CNT growth, the mechanism is termed vapor-solid-solid (VSS).[77, 83] Compared to the latter, the former catalysts are more likely to be destabilized, thus making it hard to obtain uniform or homogenous CNT structures. More discussions on the VLS and VSS mechanism can be seen in other reviews and books.[67, 84]

As for carbon adsorptions on catalyst surface, an increasing number of *in situ* TEM studies have pointed out that carbon adsorptions on the catalyst surface influence the stability of catalysts, such as the discussions on surface-bounded catalyst dynamics,[43] carbon-involved dynamical evolutions of catalysts,[57] and carbon-involved near-surface evolution of Co nanoparticles on CNT diameter and growth modes.[85-87] The structural or morphology evolutions of catalysts can then drive CNT nucleation and influence CNT growth.[88, 89] See more in Section 3.1.2 for the substrate effect on catalyst stability.

3.1.2 Interactions of Heterogeneous Interfaces

The most essential information for CNT growth is the size correlation between catalysts and CNTs. The diameter of a CNT is either similar with particle size or smaller than that, so called tangential and perpendicular growth modes (Figure 4a). It is generally accepted that the tangential growth mode is the dominant mode and therefore CNT diameter can be defined by the particle size. The atmospheric-pressure E-Cell results from our group all demonstrate this mode when there is sufficient carbon supplies (Figure 4b).[58] While *ex situ* TEM results demonstrated that the two growth modes might evolve as growth period,[90] which is in accordance with the statistical trend under ETEM from Sharma's group (Figure 4c).[87] Based on the ETEM and CVD results, Yang *et al.*[86] proposed that the growth modes of SWCNT from Co and Co-W alloy catalysts depend on physical state of catalysts (Figure 4d-e). More tunable growth conditions and observations during the whole growth stages of a CNT are needed to address the apparent disagreement.

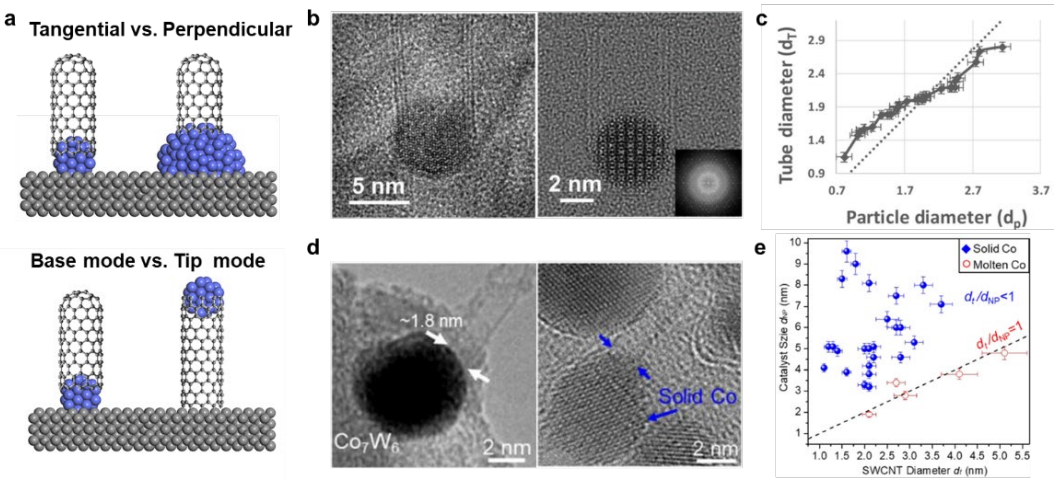

Figure 4. Growth modes showing the heterogeneous interfacial correlations between catalyst and CNT. (a) The schemes of tangential and perpendicular growth modes, base and tip growth modes. (b) The captured TEM images showing the tangential mode under atmospheric-pressure E-cell.[58] (c) The size correlation based on statistical data from ETEM growth results.[87] (d) The perpendicular mode from solid catalysts and (e) statistical data for two growth modes depending on the physical state of nanoparticles.[86]

For a long term, it has been conceptually conceived that it is achievable to control SWCNT structures by fabricating nanoparticle with proper size and structures via epitaxial growth, while only post-growth TEM characterizations confirmed that there are correlations between the crystallographic orientation of catalyst particle and CNTs.[91, 92] It is not easy to study the geometrical fit between a CNT and catalyst surface. By *in situ* investigating the growth of SWCNTs from platelet boron nitride nanofiber, we demonstrated that a SWCNT can hetero-epitaxially nucleate from the open (002) edges of the boron nitride (Figure 5a), and the diameters of the SWCNTs are multiples of the BN (002) interplanar distance.[93] For multi-wall CNTs, the structural analysis after growth suggested no epitaxial relationship,[94] so as to high-melting point Co-W catalysts for *in situ* growth of CNTs,[58] see more in Section 3.3.2. The epitaxial growth is still an intriguing topic but more considerations such as the cleanness at nanotube-catalyst interface[95] and special catalyst systems are needed.

In addition to the catalyst-CNT interface, catalyst-substrate interface also plays an important role in CNT growth, which determines the base or tip modes of CNT growth (Figure 4a). For tip growth modes, catalysts with weak connections to the substrate tend

to detach from the substrate during CNT growth. Conversely, for base-growth there is a strong catalyst-substrate connection. As evidenced by ETEM, parameters that can affect the interactions of catalyst-substrate interface, such as temperature[96] and catalyst preparation method,[97, 98] can also influence the CNT growth modes and even the selectivity results.

Besides, there is a complex catalyst-substrate interaction under certain gas environment, and the stronger the interaction at catalyst/substrate interface, the better the preservation of nanoparticle facets or activity.[43, 99] The catalyst-substrate interactions also affect the formation of carbon layer under certain carbon sources,[100] the thermal stability[101] and catalyst composition[102]. Interestingly, He *et al.* realized the epitaxial formation of monometallic Co nanoparticles with well-defined crystal structure from MgO support (Figure 5b),[98] which is a possible reason for the chiral-selective growth of SWCNTs. In addition, the catalyst-support interaction for tunable catalytic behaviors is a widely investigated topic in catalysis, involving a variety of catalyst systems. An in-depth understanding of the interactions under CNT growth conditions will provide more insights into catalyst design, controlled CNT growth and CNT growth termination.

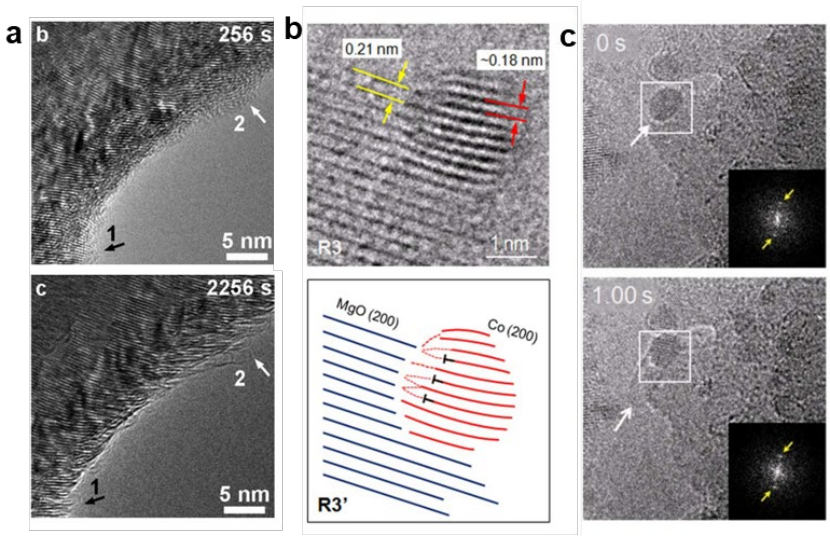

Figure 5. *In situ* TEM revealing the epitaxial relationships between catalyst and CNT, as well as catalyst and support. (a) A SWCNT hetero-epitaxially nucleates from the open (002) edges of the boron nitride nanofiber.[93] (b) The formation of Co catalyst nanoparticle epitaxially from MgO support and (c) the *in situ* growth a SWCNT.[98]

3.1.3 Kinetics under Reactive Conditions

To gain insight into the growth kinetics of catalyst and CNTs, a sequence of BF-TEM images with time and conditions (temperature and pressure) resolved data are normally used to follow the evolution processes. CNT growth kinetics involves incubation, nucleation, growth and growth termination kinetics, influenced by kinetic factors such as temperature, carbon concentration, reaction time, etc.

Owing to the high-temporal resolution, *in situ* TEM is also capable of obtaining quantitative information about the earliest period of CNT nucleation where total CNT length is within a few tens of nanometers. For instance, the incubation time for CNT nucleation, i.e., the time from the formation of nanoparticle after carbon introduction to nucleation of a CNT, can be identified[103], which are varied as particles with a minimum value of 4 s. The followings are mainly on evolution kinetics of catalyst during CNT growth and conditions on CNT growth kinetics.

The carbon diffusion paths and diffusion kinetics towards catalysts are believed strongly related to the chemical and physical state of catalyst. Recently, Lin *et al.*[104] observed dynamic phase transformations in a Co catalyst nanoparticle at atomic scale when a low pressure of C_2H_2 (0.01 Pa) at 650 ℃ is provided under ETEM (Figure 6a). They developed a method on the determination of the atomic-column positions of particles from a sequence of high-resolution images.[105] Then, two distinct regions with different structures (R1 and R2) and a clear boundary can be visualized. By measuring lattice spacings and angles from the fast Fourier transforms of the high-resolution images, metallic Co and Co_2C structures were identified for the two regions (Figure 6b-c). For the first time, it has been evidenced that the co-existence and the dynamic fluctuations of two active phases in a particle during CNT growth. It was also proposed that instead of the commonly believed surface or sub-surface diffusion of carbon on a solid catalyst, the carbon diffusion pathway may involve the entire catalyst particle via the fluctuations in the formation and decomposition of metastable phases. The fluctuations in catalyst carbon content are quantified and inversely related to carbon incorporation rate to CNT (Figure 6d-e). These atomic scale results confirmed that carbon gradient can act as a driving force for carbon diffusion, in contrast to the previous mechanism that the driving force of carbon diffusion is temperature gradient.[106]

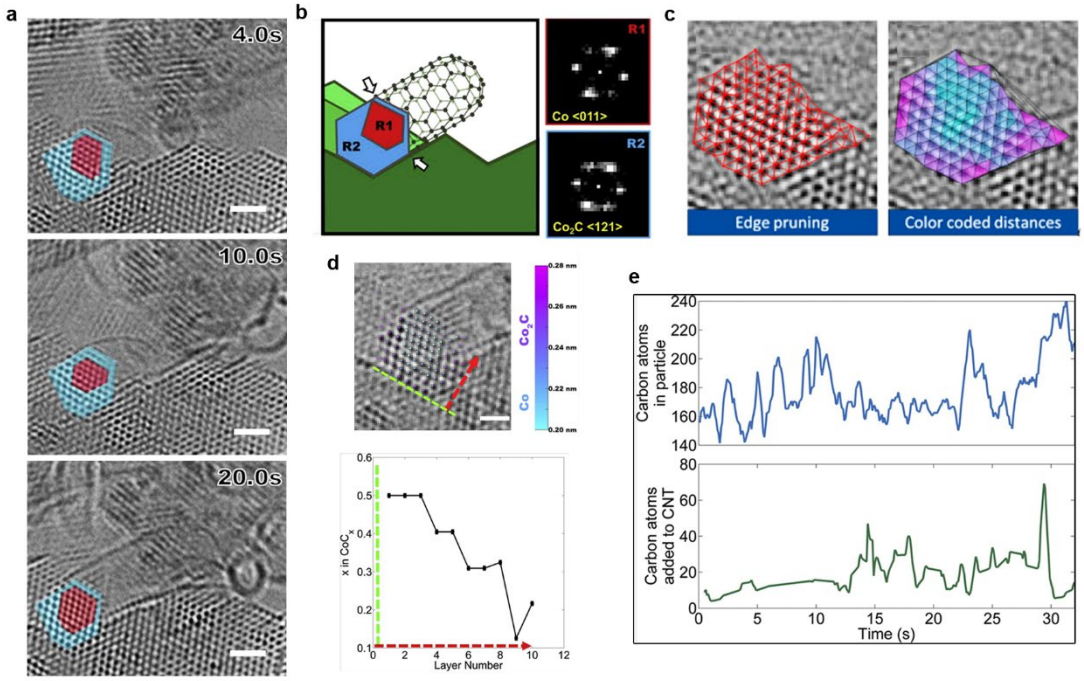

Figure 6. *In situ* TEM measurement of the carbon content in Co nanoparticle and the growing SWCNT.[104] (a) High-resolution TEM images of CNT growth and the dynamic fluctuations of Co and Co_2C domains. (b) The illustration of the identifying catalyst particle with the Co and Co_2C structures in R1 and R2, respectively. (c) Image processing scheme method for accurate assignment of atomic columns as Co or Co carbide phase.[105] (d-e) The spatial and temporal variations in carbon content in the catalyst particle and the growing SWCNT.

Kinetic parameters such as temperature, pressure and type of carbon precursors were *in situ* demonstrated to influence CNT growth kinetics[107-109] which may take effect by changing carbon diffusion path or rate towards catalyst particles. By observing a multi-wall CNT growth at a controlled temperatures on Fe catalyst particles, Gamalski *et al.*[110] presented a length (growth rate) instability of multi-wall CNTs mainly at low temperature. They clarified the rate-limiting step to the limited diffusion of carbon atoms across the CNT outer walls and through large particles. See more instable growth of CNTs in section 3.3.2. Regarding gas pressure, Sharma demonstrated under ETEM that the higher the gas pressure, the faster the growth of CNTs.[111] With studies of both ETEM and CVD growth of SWCNTs, a strong linear relationship between CNT growth rate and the active catalyst surface/tube diameter ratio was developed by He group,[107] so that SWCNTs with a specific chirality were selectively controlled on the basis of kinetic theory. They also proposed that the classical screw dislocation model[112] for

SWCNT growth kinetics and chirality control only works when there are enough etching agents in the environment, otherwise the growth rate of SWCNT is structure independent. For collective nanoparticle evolution kinetics and CNT growth kinetics, both series of TEM images and EELS acquired during CNT growth can be used to monitor the surface carbon accumulation in the form of CNTs and the termination of CNTs.[103]

3.2 CNT Nucleation Mechanism

The *in situ* dynamic study of SWCNT nucleation and growth under realistic condition is very challenging, especially for the early stages of nucleation. In the past decades, much progress has been made in revealing nucleation mechanisms of CNTs especially SWCNTs by means of *in situ* TEM. Here we will review the topic by clarifying driving forces for CNT nucleation, identifying nucleation sites for a SWCNT and developing some new understandings.

3.2.1 Driving Forces for CNT Nucleation

It is generally believed that the nucleation consists of the sp^2-carbon cap formation and its lift-off from a catalyst particle. Several *in situ* TEM investigations of CNT nucleation have provided important insights on why a CNT nucleates. Among these, the driving force for CNT nucleation is the fundamental question to understand the formation of CNTs.

As for the scenario of cap formation, it seems necessary that a metal tip firstly deformed from a flat/facet surface to a convex/round one, then a hemispherical cap forms by replicating the shape of the apex of metal particles due to a wetting effect by the carbon surface layer.[113] Even for a faceted catalyst, a cone-shaped cap might also follow the shape of catalyst particle by a post-characterization.[91] In most cases, small catalyst particles keep aspherical shape at high temperature, such as Au catalyst, so that sp^2 carbon shell is gradually assembled on the surface, and the carbon cap lifts off from the fluctuating particle surface.[114] The above scenario revealed by CNT-cell or *ex situ* TEM is the classical yarmulke mechanism for a CNT nucleation, in which a hemispherical cap forms on the catalyst particles and lifts off to nucleate closed CNTs.[115] Later, *in situ* ETEM experiment results have also proved the mechanism (Figure 7a).[43, 44]

The surface energy anisotropy of catalyst as a driving force for CNT nucleation was

evidenced and quantitatively calculated by Pigos *et al.*[116] by *in situ* observing the morphology evolution of catalysts. It was revealed that catalyst morphology evolved to a spherical shape if carbon atoms partially chemisorbed on the surface of it, which then reduces the surface energy anisotropy. Once the sp^2-carbon dome formed, the particle surface tends to be flattened and increases surface energy anisotropy, resulting in the lift-off of the sp^2-carbon cap. So far, it is widely accepted that the catalyst morphology oscillations drive the cap detachment from the particle. In addition, some other factors or ways may contribute to the SWCNT nucleation, such as surface energy evolutions due to catalyst interfacial step flow,[74] the near surface lattice expansion of a catalyst nanoparticle[17, 85] or the evolution of atomic structure of ultrasmall nanocrystals.[61]

3.2.2 Nucleation Sites of SWCNTs

It is generally believed that nucleation site represents the active site for a cap formation and lift-off for a CNT. So far, only heterogenous nucleation of CNTs from catalyst nanoparticles was *in situ* observed, therefore, it is necessary to capture the evolution dynamics of catalyst and catalyst/tube interface at the very beginning of CNT nucleation and identifying nucleation sites.

Helveg et al.[73] for the first time pointed out the Ni step edges as growth centers were coupled to graphene sheets during the formation process of a carbon nanofiber, due to the favorable carbon binding energy to the step edge. Later on, by considering the catalyst-SWCNT interface and interactions, Zhu and Iijima et al.[91] realized the atomic resolution of step edges as nucleation sites for a cone-shaped cap by ex-situ high-resolution TEM. They additionally confirmed that the positions of step edges determine the diameter of a SWCNT, and proposed that the step sites are supposed to form during CNT nucleation and growth. While more details on the dynamic process and the way carbon incorporation into a cone-shaped cap are still up in the air.

On this basis, *in situ* evidences are required to address the open question whether catalyst with controlled steps can be designed and then contribute to the growth of SWCNTs with specific chirality. Rao *et al.*[74] performed *in situ* ETEM experiment and correlated the carbon adsorption to the surface reconstruction of Ni catalyst particle through step flow. In details, the graphene embryo is bound between opposite step edges on the Ni particle surface, as step edges migrate through the adjacent facets towards the open end of particles, the curved cap formed and lift-off. Owing to that, the authors stressed that catalyst geometries from the view of 3D rather than only one facet, such

as the interfacial angles between the adjacent facets on catalysts are important for CNT nucleation and might take effect in tuning cap curvature and determine the chirality. The dynamic formation and evolutions of step sites during CNT nucleation have been studied in more detail. Recently, we have observed *in situ* nucleation of a SWCNT from a solid Pt catalyst at 550 °C under ETEM, and found that a cap tangentially extended from the particle with its lift-off to the length of around 1 nm.[117] During the process, the embryo SWCNT fluctuated its length with time possibly due to the fast motion of step edges. Except for that, during the extension process of the SWCNT, Pt particle formed a step edge at one side, which then took as active sites for the asymmetrical elongation of the SWCNT and produced the alteration of chirality. These direct evidences confirmed that the atomic step edges are active sites for carbon incorporation, can form and evolve under bounded carbon layer and gaseous conditions.

In addition to the step-mediated formation of a cap, there are also new understandings on the cap formation scenario during SWCNT nucleation. Different from Rao's study, Sharma *et al.*[70, 99] consider the facet effect either as anchoring or lift-off sites. They directly observed a graphene embryo covered on the corner of two surfaces of Co_2C, then spread over only one surface and be anchored to the other surface under ETEM (Figure 7b). Adjacent surfaces with dissimilar works of adhesion were calculated for catalyst particles to convert a graphene into a hemispherical cap and lift-off to a SWCNT. Essentially, the differences were attributed to the different termination atoms, either with Co-C or Co.

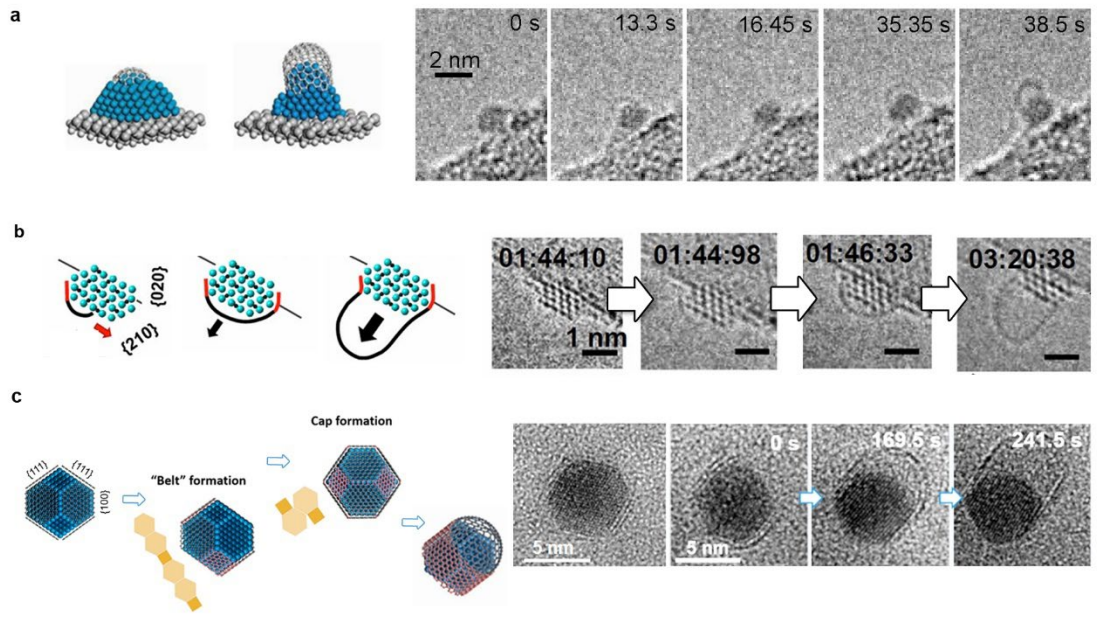

Figure 7. Nucleation mechanisms of SWCNTs under reactive conditions. (a) The classical yarmulke mechanism for a CNT nucleation.[43, 44] (b) A cap nucleation converted from a graphene on a Co catalyst.[99] (c) A "belt" mechanism for SWCNT nucleation.[81]

3.2.3 Nonclassical CNT Nucleation Mechanisms

Although it was assumed that the carbon cap was formed and lift-off from catalysts, which then dictate the helicity of a SWCNT, CNT nucleation is a very complicated dynamic process, it is still too early to tell whether nucleation process determines CNT diameter or even chirality. Therefore, more investigations are needed to deepen the understanding of CNT nucleation and provide more insights for catalyst design and optimization of growth conditions. We will here introduce some recent advances on the nonclassical nucleation that may offer possibilities for structural control of CNTs.

For the mass production of SWCNTs by floating catalyst CVD, assisted catalysts or promoters such as sulfur play a crucial role on the formation of localized nucleation sites of catalysts, whose size would determine the diameter and wall number of CNTs. We have clearly demonstrated by *in situ* TEM that a CNT can grow tangentially from a pure Fe catalyst, while with the addition of sulfur, small SWCNTs can grow from inhomogeneous local active sites of Fe catalysts and keep the diameter smaller than particle size, i.e., in a perpendicular mode.[118] The promotion effect may originate from the modification of interface bonding between catalysts and precipitated graphitic layers, which requires more experimental and theoretical studies.

It is generally agreed that a catalyst particle only nucleate one SWCNT, as observed in most *in situ* TEM experiments,[43] except for several multi-wall CNT growth[110] or inner wall nucleation of multi-wall CNT from the same particle.[116] Recently, we have for the first time observed the multiple nucleation of SWCNTs and termination progress from an individual catalyst under ETEM,[119] which evidenced the changes of interfacial structures during the detachment of the first SWCNT and the second nucleation from the same particle, as well as the concentric nucleation of each wall for a multi-wall CNT. Different from the prior understanding in the reference[116] that apparent shape oscillation and movement of particles within a nanotube cell drives the repeated nucleation, the SWCNT nucleated directly from the small particle appears to oscillate less and remain active for the next nucleation after the termination of the first nucleation. It has been recently shown that several SWCNTs can nucleate from different sites of a

particle,[62] and whether the produced SWCNTs will maintain similar structural gene needs to be further investigated. The multi-nucleation of SWCNTs was confirmed by atmospheric-pressured floating catalyst CVD results,[120] presenting a general mechanistic understanding for yield improvement and possible structure control.

Recent progress in controlling chirality of SWCNTs was attributed to the good thermal stability and geometry of high melting-point catalyst, however, the nucleation mechanism of individual SWCNTs from faceted catalyst remains lack of detailed knowledge. Because catalyst particles for CNT growth are usually in a liquid-like spherical shape, Smalley *et al.* came up with the "yarmulke" model, that is, hemispherical carbon cap from a sp^2 carbon on the surface of the catalysts. Theoretical calculations predict that the initial cap determines the chirality of successive growing CNTs. The reported faceted catalysts also seem to follow the classical one-step nucleation based on the yarmulke model.[74, 99]

Recent *in situ* TEM studies show that several graphene layers grew simultaneously on Pt nanoparticles, indicating that a SWCNT may nucleate in a different way from a well-faceted Pt catalyst. Indeed, a truncated octahedral Pt nanoparticle was *in situ* prepared at atmospheric pressure and took as a model catalyst, it was found that in the early stage of CNT nucleation, graphene formation on the particle was facet-dependent. The initial nucleus consists of a cap and an annular carbon belt by joining several graphene layers from faceted Pt catalysts particle, we term it "belt" mechanism, as summarized in a 3D nucleation model (Figure 7c).[81] It is the belt rather than the cap guiding the subsequent CNT growth, indicating a possible chirality control mechanism based on the facet-dependent nucleation and growth of SWCNTs from a catalyst with an anisotropic surface energy.

3.3 CNT Growth Mechanism

CNT elongation becomes easier once a CNT nucleates and more carbon atoms are continuously supplied. During CNT growth process, the state of catalyst particles and the structure of CNTs shall be tracked and analyzed, so that *in situ* TEM studies especially atmospheric-pressure ETEM show advantage in providing valid evidences for an in-depth understanding of CNT growth mechanism, compared to post-growth characterization and other *in situ* techniques. Two decades ago, the growth of CNTs can be realized inside TEM and *in situ* observed.[121] So far, several issues were investigated and clarified such as the active phase and evolution dynamics of catalyst during CNT

growth (Section 3.1.1). So that a clearer picture of CNT growth mechanism can be seen, such as the diffusion pathways of carbon atoms; the observation of CNT growth process and measurement of CNT growth rate; the determination and control over CNT growth rate-limiting steps (correlating the CNT growth kinetics to the growth parameters); the variations of CNT growth rate as a function of the growth temperature, catalyst type or state, reaction gas, and pressure. Upon well understanding the growth mechanism, it is possible to propose strategies to boost the growth and to obtain CNTs with controlled structures.

3.3.1 Catalyst Structure-Related Fluctuated Growth of CNTs

To learn about the growth kinetics of individual CNTs, the measurement of instantaneous CNT growth rate is necessary, which is strongly dependent on the ability to identify each step in a reaction. Lin *et al.*[122] followed the growth process of a SWCNT and claimed that the growth rate of individual CNT can be divided into slow, rapid and decay regimes as time even without changes of growth conditions (Figure 8a-b). However, the direct measurement of an unsupported SWCNT as long as 50 nm is still hard, the thermal vibration and flexible property of SWCNTs make the images unclear. So, a reliable measurement method of a long SWCNT is still needed. Again, the rough measurement of the growth rate at a relatively low magnitude can hardly be correlated to the structure of catalysts.

For a flying multi-wall CNT or fiber structures, the TEM projected length is used to estimate the growth rate although it is claimed underestimated and correction factor is needed.[111] With this method, Sharma *et al.*[123] compared the growth kinetics of different CNTs and found that under the same temperature and pressure, CNTs with nearly same diameter grew at different rates. To clarify the discrepancy, it is necessary to obtain growth rates of multi-wall CNTs by measuring tube length, diameter and wall number, and then calculate the number of atoms added per second.

An ideal *in situ* TEM experiment is able to give reliable information on the size and composition of catalyst particle, the CNT length, diameter and wall number, the time duration of growth, and the start time for CNT growth after introducing carbon source. Compared to the *in situ* thermogravimetric analysis (TGA) experiments on a milligram scale, *in situ* TEM analysis of individual CNTs and catalyst particles at the nanoscale can tell more fluctuated details of carbon growth rates[124] (Figure 8c). Additionally, the contribution of controlled parameter such as catalyst nanoparticles

to the carbon growth kinetics is also allowed by *in situ* TEM. Welling *et al.* then found that the carbon growth rate and final structures (either multi-wall CNT or a nanofiber) are strongly dependent on particle size and composition, in consistent with the relationships for SWCNT growth from a small Co particle under ETEM.[104] The fluctuation in the carbon concentration in the catalyst nanoparticle and the fluctuations in SWCNT growth rates are found complementary (Figure 6e). For a Pt catalyst, the embryo SWCNT with a sub-2 nm diameter also fluctuates with time during the early stage of nucleation (Figure 8d-e),[125] suggesting a weak relationship between the SWCNT and the Pt catalyst and a possible step flow or structural changes at an unresolved rate. Note that based on the *in situ* ETEM measurement of CNT growth rates, it is reported that there is a strong linear relationship between the CNT growth rate and the exposed catalyst surface area to the tube diameter,[107] which provides new insights for the control over SWCNT chirality by designing kinetic factors.

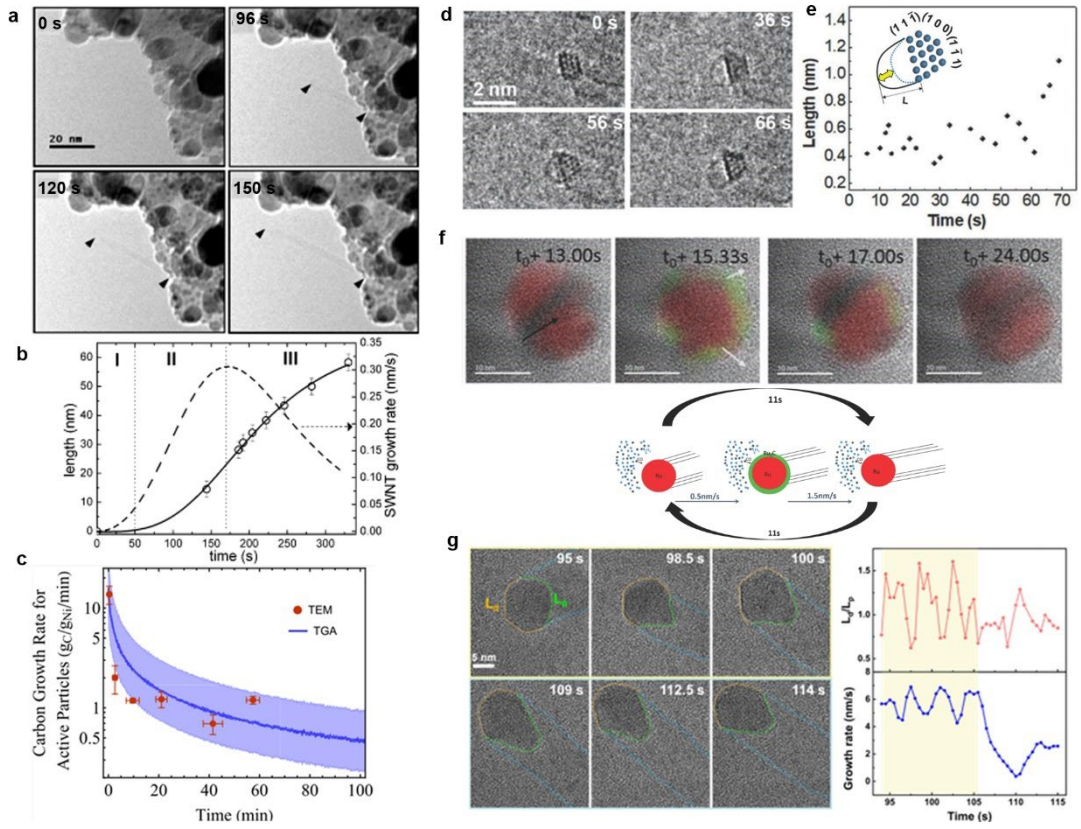

Figure 8. (a-b) TEM images showing the growth process of a CNT under ETEM.[122] (c) *In situ* TEM analysis of individual CNTs at the nanoscale can tell more fluctuated details of carbon growth rates, compared to the *in situ* TGA experiments on a milligram scale.[124] (d-e) The CNT nucleation fluctuation from a sub-2 nm Pt

catalyst.[125] (f) A “cyclic” mechanism for CNT growth from Ru catalyst particles with size evolutions and the sub-surface metal-carbide phase transition.[56] (g) Morphological changes of a Ni nanoparticle during the CNT growth and the profiles showing the structure evolutions of catalysts with the fluctuations of growth rate of CNTs.[76]

Even under atmospheric pressure ETEM with sufficient carbon supplies, the fluctuated growth of a CNT can be observed. A “cyclic” mechanism for CNT growth from Ru catalyst particles was proposed. The relaxation oscillation of the growth rate occurred along with size evolutions and the sub-surface metal-carbide phase transition of catalyst particles (Figure 8f).[56] We observed the fluctuated growth rates of CNTs and correlated them with the structure change of Ni nanoparticles (Figure 8g).[76]

The reported growth rate of CNTs measured under *in situ* TEM is usually in the range of several nanometers to tens of nanometers per second, similar to that from non-metal catalysts under CVD process. However, the normal growth of either straight-wall SWCNT or multi-wall CNTs under CVD process is in the range of nano- to micrometer per second, suggesting that diffusion of carbon atoms through/on catalyst particle should be very fast at real growth conditions. The rate-limiting factor is thus not the carbon diffusion through catalyst particle. Although it is possible to grow long and straight CNTs especially SWCNTs at fast growth rate under ETEM, to track the length of a growing CNT and to investigate its correlation with catalyst and other conditions is still far beyond the temporal resolution of the video recording system.

3.3.2 Instable Growth and CNT Structure Evolutions

Under diverse conditions tuned under ETEM or E-cells, the diameter, wall number and length of CNTs can be changed.[108] Even under constant growth conditions, it is reported that the CNT can not only change its length and growth rate as time, but also the growth direction and wall structures. The origin is related to the possible diffusion processes of the dissociated carbon atoms, catalyst and catalyst-tube interfacial evolutions during CNT growth. *In situ* TEM experiments demonstrated that the carbide catalysts remained stable during the formation of CNT, such as Fe, Co-W and Pt catalysts. Taking metallic Co catalyst as an example, after precisely identifying the active phase of Co catalysts as carbide under atmospheric pressure, the carbon diffusion path was determined to diffuse at the surface of the catalyst or at the catalyst-tube

interface (Figure 3d).[37] The inhomogeneous structures of Co-Pt catalysts,[109] similar to the inhomogeneous catalysts containing both Co and Co carbide,[126] might trigger different CNT growth rates and were proposed to follow bulk and sub-surface diffusion.

The observed CNTs under ETEM are normally defective, such as bended, which might lead to the fluctuation behaviors of CNTs proposed by Sharma.[111] Although they conjected that the bends are related to the change in growth direction that is dictated by the crystallographic orientation of Ni catalyst particle, direct evidence is still absent. Hofmann *et al.*[43] believed the formation and inclusion of defect structures due to the faster carbon supplies than the defect healing process at low temperature. Yoshida *et al.*[127] for the first time demonstrated that the deformation of catalyst nanoparticles during the growth of multi-wall CNTs triggers the formation of various defects such as bends and disorder of the interlayer spacing in CNTs. With the observation of atomic structure of Pt nanoparticles, we firstly correlated the formation of atomic steps during SWCNT growth to the formation of topological defects along the SWCNT wall (Figure 9a).[117] In addition, ETEM is also a powerful tool to study the mesoscale dynamics of CNT networks, it is found that the tube-tube mechanical coupling can alter their growth trajectory and cause significant buckling, bending and other defects of CNTs during growth of a dense network.[128]

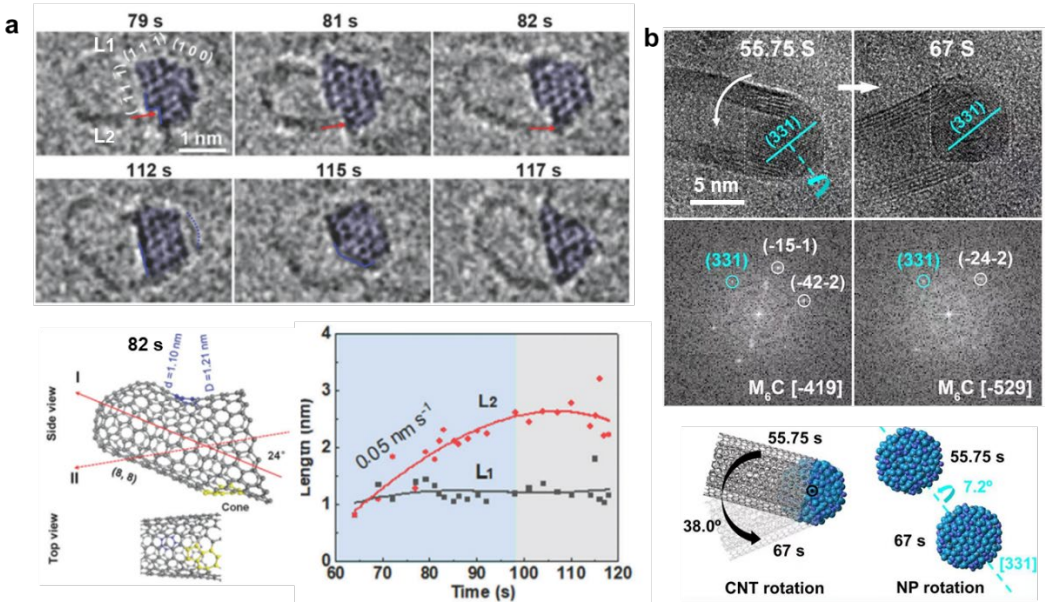

Figure 9. Instable growth of individual CNTs. (a) Asymmetric growth of a SWCNT from an atomic step site and the changes in the catalyst-SWCNT interface formed by step movement.[117] (b) Rotation of a CNT around Co-W-C alloy catalyst nanoparticle during CNT growth.[58]

Recently, the growth direction change of CNTs was demonstrated no correlation with the crystallographic orientation of catalyst particle, even for a solid alloy catalyst (Figure 9b).[58] Under atmosphere pressure, we have demonstrated that although the particles changed their crystal orientation during CNT growth, the growing SWCNT or multi-wall CNTs rotated around Co-W-C alloy catalyst particles independently. The weak interfacial interaction between the solid catalyst and the growing CNTs suggests that it is difficult to achieve the structure-controlled growth of CNTs solely relying on the template effect of solid catalyst.

3.4 Termination of CNT growth

3.4.1 Controversaries on the Growth Termination of CNTs

In general, catalysts are attached to the tube during CNT growth and form bonds at the growth front to prevent the closure of CNT open edges. Instead, growth termination is the process of disrupting the continuous incorporation of carbon dimers at the catalyst-tube interface, which is generally believed the result of activity depletion of catalyst.

Understanding the growth termination mechanism of CNTs may lead to the growth of CNTs with infinite length, i.e. greatly improved yield, or shed light for the control over CNT morphology and structure. Remarkable progress and evidences in the growth termination mechanisms for both individual and collective CNTs have been disclosed. We categorize them as follows: (1) catalyst poisoning for a decreased catalyst activity;[129, 130] (2) catalyst aggregation;[131] (3) catalyst morphology evolution[132] or detachment from CNT;[54, 119] (4) self-deactivation by defect accumulation at catalyst-tube interface;[133] (5) impeded carbon diffusion or broken local carbon cycle through or over catalyst particles to discontinue growth of SWCNTs.[119, 129] It can be seen that in addition to the controversaries on the ways catalyst depletes activity (1-4), environment or substrate effect on the CNT growth termination (3-5) cannot be ruled out. Thereby, in order to the control over the termination process and CNT structures, it is necessary to deeply investigate the contributions of catalysts and conditions on the CNT growth termination mechanism.

Among the previous recognitions, it is found that the objects are mainly based on a macroscale collection of CNT arrays. For instance, the abrupt termination growth mechanism of vertically-aligned CNTs as catalyst aggregation under hydrogen was ex-situ studied.[131] The growth kinetics of SWCNTs were revealed by *in situ* Raman and

suggested the capability of defect healing at the interface would determine whether growth will cease or not.[133] In most catalyst deactivation case, the introduction of water can greatly improve the activation energy for carbon incorporation. In fact, due to the complexity of CNT growth process as discussed before and insufficient details provided by optical spectroscopy or *ex situ* techniques, it is still unclear for the controversial topic.

3.4.2 Understanding of CNT Growth Termination Mechanism

ETEM provides a platform for investigating the growth termination mechanism of CNTs, several evidences for the ways CNT terminated growth or the reasons under reactive conditions have been provided. In order to explore the effect of catalyst and environment conditions on CNT growth termination, we have recorded the CNT growth dynamics and investigated CNT-catalyst interfacial structures for both individual MWCNTs and individual SWCNTs under tunable conditions by *in situ* TEM. As shown in Figure 10a, the CNTs stop growing in the way of necking or broadening CNT-catalyst interface connections. With more experimental comparisons, we propose two main reasons for the CNT cessation: insufficient active carbon species for Co catalysts and stress exerted at the tube-catalyst interface, by breaking carbon cycle through or over catalyst particles and reducing the tube-catalyst adhesion strength.[119] These understandings suggest that designing catalysts and optimizing growth conditions for a better carbon cycle through catalysts and an enhanced catalyst-CNT interfacial interaction, shall improve CNT growth length (or yield). It is in agreement with the density functional theory calculation result that Fe, Co and Ni catalysts have larger adhesion strengths to SWCNTs than Cu, Pd, Au, which are likely to be more efficient for a continuous CNT growth.[134]

In addition, conditions that affecting physicochemical properties of catalysts can also cause CNT growth termination. Both cross-section of *ex situ* TEM and ETEM results confirmed that catalyst morphological evolved through the diffusion of Fe into the sub-surface of Al_2O_3 support under high temperature, and finally detached from the end of CNTs (Figure 10b).[132] This kind of subsurface diffusion of catalyst towards the underlying support plays a fundamental role in the termination of vertically aligned CNT array growth.[132, 135] Moreover, planar Ostwald ripening of catalyst particles, temperature-induced structural evolution of catalyst support, particle coalescence can induce CNT growth termination.[136] Since reaction-induced metal-support interaction

is a widely investigated strategy modifying catalyst activity,[102] it is expected to screen a large group of catalyst systems (catalyst and support) to modulate CNT yield. Except for that, catalyst particles were also observed deactivated by detaching from the support and climbing up through CNT arrays during the growth.[89]

Huang's group demonstrated several termination mechanisms of multi-wall CNTs.[54] In addition to the weakened interface adhesion like SWCNTs, multi-wall CNT can also terminate growth by a coverage of catalyst and Ostwald ripening (Figure 10c). Rao *et al.*[74] reported the growth termination of MWCNTs either by catalyst morphology changes as a result of step flow or catalyst-tube interface evolution based on step bunching phenomenon. The former induced the formation of flattened steps and the detachment of the outer wall of CNTs, while the latter destabilized the step train by the overlayer carbon adatoms or graphene layer. These kinds of growth termination scenarios are proposed to be prevalent in special shaped nanotubes such as bamboo-like tubes and tubular multi-wall CNTs, respectively. Similar reasons due to the compressive strain relaxation of overlayer graphene[137] also work to facet a relative larger catalyst nanoparticle for the growth of carbon nanofibers.[94]

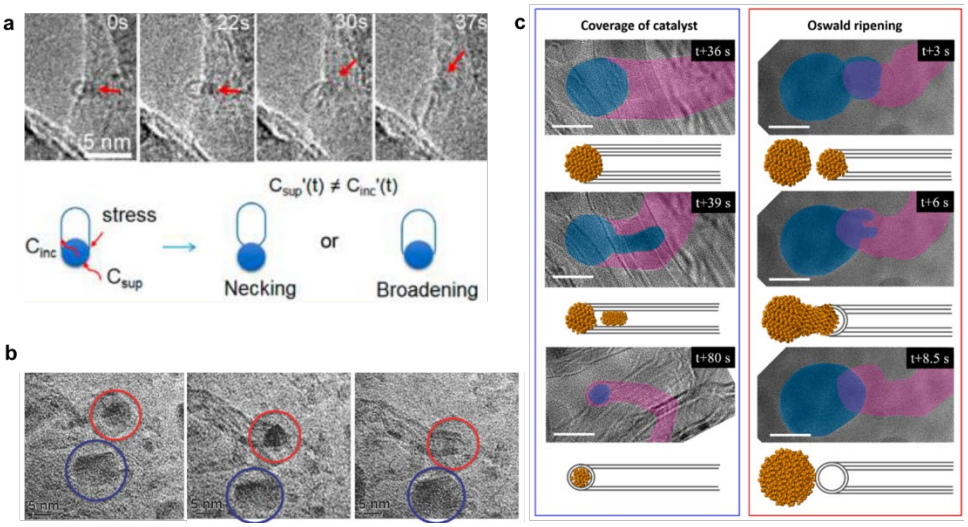

Figure 10. Growth termination mechanisms of CNTs revealed by means of ETEM. (a) The broken carbon cycle through or over catalyst particles for a SWCNT cessation.[119] (b) Subsurface diffusion of catalyst towards the underlying support terminated the growth of a CNT.[132] (c) A coverage of catalyst and Ostwald ripening termination mechanism of CNTs.[54]

To date, a deeper and more comprehensive understanding on the growth termination mechanisms of CNTs has been achieved, and it is clear that no single growth

mechanism can explain all of the features of CNT growth, especially for vertically aligned CNT arrays.[138] More direct evidences by *in situ* TEM studies are still needed to achieve a more accurate understanding of CNT growth.

4. Conclusions and Outlook

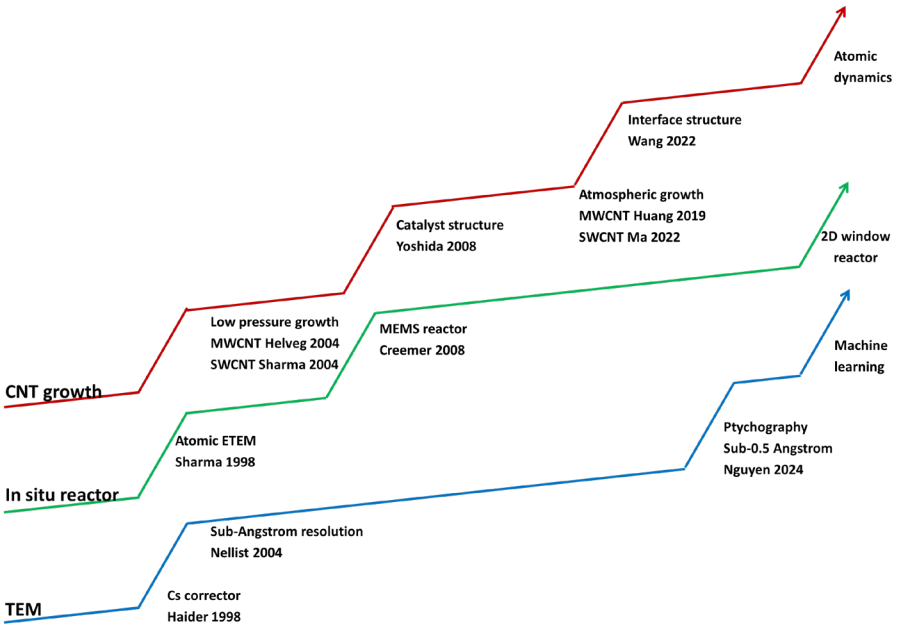

Figure XX Milestones and roadmap of in situ TEM for CNTs growth mechanism

Over the past two decades, thanks to the advances in the atomically resolved in situ environmental TEM, the black box of growing CNTs has been gradually opened, revealing valuable information regarding the nucleation and growth thermodynamics and kinetics. A series of *in situ* TEM reactors have been developed to realize and in real time monitor the growth of CNTs under TEM, during which crystalline structures of catalysts and interface dynamics during CNT growth have been characterized and tracked. Important questions on the growth of CNTs, such as the facet dependent nucleation, state and phase of active catalysts, dynamic interface interactions between catalyst and growing CNTs, have been clarified.

However, there are still open questions and great challenges remained. Currently, most researches have been focusing on the state of the catalysts, while the structural dependence between the atomic structure of catalysts and fine structures of CNTs is still missing.

Regarding the technical aspects of *in situ* TEM for investigating the growth mechanism of CNTs, a primary technical difficulty is to characterize the atomic

structure of CNTs in a gaseous environment and under the influence of membrane windows for the E-cell reactors. Because of the small mass of carbon atoms, signals from the interaction between electron beam and CNTs are much weaker than those from heavy metal atoms, such as the catalysts. In addition, it takes about 1 second to take a conventional TEM image, while atomic dynamics are in the range of femtoseconds to nanoseconds. Furthermore, in contrast to the three-dimensional periodic crystalline structure, CNTs have a unique circular geometry in cross-section. It is still very challenging to characterize such complex structures with atomic resolution. A final technical challenge is the inevitable structural fluctuations for the nanostructures at a high temperature and under electron beam irradiation.

The purpose of *in situ* study on the growth mechanism of CNTs is to understand the atomic dynamics under the real growth conditions. And based on the revealed growth mechanisms, the ultimate goal is to design and control the atomic structures, including the chirality, junction, and defects of CNTs to fulfill the requirement of their application in various functional devices. In the following, we give an outlook of the *in situ* ETEM study to tackle the mentioned challenges in understanding the growth mechanisms of CNTs and ultimately to precisely control their atomic structures.

(1) To tackle the challenge of atomic resolution characterizations of CNTs under growth condition, it is crucial to develop ultra-thin membranes for the reactor cells to enhance the signal-to-background ratio. One candidate is the two-dimensional materials such as mechanically strong and chemically stable h-BN based atomically thin membranes.

(2) To bridge the gap between the time of growth reactions and TEM imaging, one promising direction is to apply ultra-fast TEM techniques with a temporal resolution of picoseconds and even femtoseconds to capture the atomic dynamics such as the chemical reaction paths.

(3) Regarding the challenge of circular interfacial structures of CNTs, atomic resolution electron tomography using STEM has been recently demonstrated a key technique for resolving 3D atomic-scale structures of nanocrystals. For CNTs of light carbon element, STEM-Ptychography based tomography is a promising solution to achieve ultra-high resolution and high dose efficiency of imaging.

(4) Finally, instead of static analysis, statistical analysis will be the solution for analyzing the highly fluctuated structures to establish the dependence pattern of atomic

structures of CNTs on the catalyst structures in a dynamic manner. For such a purpose, it is indispensable to develop AI-driven automated experiments, combining data analysis, predictive modelling and feedback control.

It is worth looking back for the milestones of in situ TEM investigations on CNTs growth mechanism that were enabled by progresses in TEM and in situ reactors, as shown in Figure XX. The most important invention was the aberration corrector which enhanced the imaging resolution to sub-Angstrom even at a relatively low accelerating voltage of 80 kV. Recently, sub-0.5 Angstrom resolution was realized by applying STEM ptychography. Another important invention is the in situ reactor. Lattice-resolved observations were realized in the 1990s, leading to the success of in situ growth of MWCNTs and SWCNTs. Atmospheric pressure was realized by applying MEMS technology to fabricate ECell-type reactors, leading to the success of atmospheric pressure growth of CNTs.

It can be expected that the in situ observation resolution will be further improved by applying advanced electron microscopy techniques such as Ptychography and machine learning. In addition, the atomically small thickness of 2D materials based reactors will allow to investigate not only the atomic structures but also the atomic dynamics during CNTs growth.

We believe with further development of advanced *in situ* TEM equipment and technology, breakthroughs in the fundamental understanding of CNT growth mechanisms can be expected. And it will be surely essential to realize the structure/property-controlled growth of CNTs and to boost their critical applications.

Acknowledgements

L. Zhang and D. M. Tang contributed equally to this work. This work was supported by the National Key Research and development Program of China (Grant No. 2022YFA1203303), National Natural Science Foundation of China (Grant Nos. 52130209, 52188101, 51927803), Key Basic Research Project of Shandong Province (ZR2019ZD49). JSPS Kakenhi (Grant Nos. JP25820336, JP20K05281, JP23H01796), JST-FOREST Program (Grant No. JPMJFR223T), WPI-MANA ‘Challenging Research Program’, NIMS ‘Support system for curiosity-driven research’, and "Advanced Research Infrastructure for Materials and Nanotechnology in Japan" of the Ministry of Education, Culture, Sports, Science and Technology (Grant No. JPMXP1224NM5238).

Received: ((will be filled in by the editorial staff))

Revised: ((will be filled in by the editorial staff))

Published online: ((will be filled in by the editorial staff))

Conflict of Interest

The authors declare no conflict of interest.

Keywords

Carbon nanotube, growth mechanism, catalyst, microstructures, *in situ* TEM

[1] S. Iijima, Nature 1991, 354, 56.

[2] R. Rao, C. L. Pint, A. E. Islam, R. S. Weatherup, S. Hofmann, E. R. Meshot, F. Wu, C. Zhou, N. Dee, P. B. Amama, J. Carpena-Nuñez, W. Shi, D. L. Plata, E. S. Penev, B. I. Yakobson, P. B. Balbuena, C. Bichara, D. N. Futaba, S. Noda, H. Shin, K. S. Kim, B. Simard, F. Mirri, M. Pasquali, F. Fornasiero, E. I. Kauppinen, M. Arnold, B. A. Cola, P. Nikolaev, S. Arepalli, H.-M. Cheng, D. N. Zakharov, E. A. Stach, J. Zhang, F. Wei, M. Terrones, D. B. Geohegan, B. Maruyama, S. Maruyama, Y. Li, W. W. Adams, A. J. Hart, ACS Nano 2018, 12, 11756.

[3] A. Javey, J. Guo, Q. Wang, M. Lundstrom, H. Dai, Nature 2003, 424, 654.

[4] X. Zhang, X. Lei, X. Jia, T. Sun, J. Luo, S. Xu, L. Li, D. Yan, Y. Shao, Z. Yong, Y. Zhang, X. Wu, E. Gao, M. Jian, J. Zhang, Science 2024, 384, 1318.

[5] R. Xiang, T. Inoue, Y. Zheng, A. Kumamoto, Y. Qian, Y. Sato, M. Liu, D. Tang, D. Gokhale, J. Guo, K. Hisama, S. Yotsumoto, T. Ogamoto, H. Arai, Y. Kobayashi, H. Zhang, B. Hou, A. Anisimov, M. Maruyama, Y. Miyata, S. Okada, S. Chiashi, Y. Li, J. Kong, E. I. Kauppinen, Y. Ikuhara, K. Suenaga, S. Maruyama, Science 2020, 367, 537.

[6] D.-M. Tang, V. Erohin Sergey, G. Kvashnin Dmitry, A. Demin Victor, O. Cretu, S. Jiang, L. Zhang, P.-X. Hou, G. Chen, N. Futaba Don, Y. Zheng, R. Xiang, X. Zhou, F.-C. Hsia, N. Kawamoto, M. Mitome, Y. Nemoto, F. Uesugi, M. Takeguchi, S. Maruyama, H.-M. Cheng, Y. Bando, C. Liu, B. Sorokin Pavel, D. Golberg, Science 2021, 374, 1616.

[7] J. R. Sanchez-Valencia, T. Dienel, O. Groning, I. Shorubalko, A. Mueller, M. Jansen, K. Amsharov, P. Ruffieux, R. Fasel, Nature 2014, 512, 61; S. Zhang, L. Kang, X. Wang, L. Tong, L. Yang, Z. Wang, K. Qi, S. Deng, Q. Li, X. Bai, F. Ding, J. Zhang, Nature 2017, 543, 234.

[8] F. Yang, X. Wang, D. Zhang, J. Yang, D. Luo, Z. Xu, J. Wei, J.-Q. Wang, Z. Xu, F. Peng, X. Li, R. Li, Y. Li, M. Li, X. Bai, F. Ding, Y. Li, Nature 2014, 510, 522.

[9] 2015.

[10] K. Otsuka, R. Ishimaru, A. Kobayashi, T. Inoue, R. Xiang, S. Chiashi, Y. K. Kato, S. Maruyama, ACS Nano 2022, 16, 5627.
[11] V. I. Artyukhov, E. S. Penev, B. I. Yakobson, Nat Commun 2014, 5, 4892; C. A. Eveleens, A. J. Page, The Journal of Physical Chemistry C 2019, 123, 10622.
[12] K. A. Dick, Mrs Bull 2023; F. Tao, P. A. Crozier, Chem Rev 2016, 116, 3487; S. Dai, W. Gao, S. Zhang, G. W. Graham, X. Pan, MRS Communications 2017, 7, 798.
[13] H. Zhao, Y. Zhu, H. Ye, Y. He, H. Li, Y. Sun, F. Yang, R. Wang, Adv Mater 2022, n/a, 2206911.
[14] Y. Jiang, Z. Zhang, W. Yuan, X. Zhang, Y. Wang, Z. Zhang, Nano Research 2018, 11, 42.
[15] V. Jourdain, C. Bichara, Carbon 2013, 58, 2.
[16] M. V. Kharlamova, Beilstein J. Nanotechnol. 2017, 8, 826.
[17] X. Zhao, S. Sun, F. Yang, Y. Li, Accounts Chem Res 2022, 55, 3334.
[18] H. Wang, Y. Yuan, L. Wei, K. Goh, D. Yu, Y. Chen, Carbon 2015, 81, 1.
[19] A. J. Page, F. Ding, S. Irle, K. Morokuma, Rep Prog Phys 2015, 78, 036501; X. Wang, M. He, F. Ding, Mater Today 2018.
[20] T. W. Hansen, J. B. Wagner, R. E. Dunin-Borkowski, Mater Sci Tech-lond 2010, 26, 1338.
[21] S. W. Chee, T. Lunkenbein, R. Schlögl, B. Roldán Cuenya, Chem Rev 2023, 123, 13374; Y. Pu, B. He, Y. Niu, X. Liu, B. Zhang, Research 2023, 6, 0043; J. Qu, M. Sui, R. Li, iScience 2023, 26, 107072; H.-Y. Chao, K. Venkatraman, S. Moniri, Y. Jiang, X. Tang, S. Dai, W. Gao, J. Miao, M. Chi, Chem Rev 2023, 123, 8347; J. R. Jinschek, S. Helveg, L. F. Allard, J. A. Dionne, Y. Zhu, P. A. Crozier, Mrs Bull 2024, 49, 174; M. Xiao, H. Sun, Y. Meng, F. Zhu, Catalysis Science & Technology 2024, 14, 2040; K. A. Dick, Mrs Bull 2023, 48, 833.
[22] R. R. Unocic, E. A. Stach, Mrs Bull 2023, 48, 828.
[23] C. S. Allen, A. W. Robertson, A. I. Kirkland, J. H. Warner, Small 2012, 8, 3810.
[24] G. M. Vanacore, R. M. van der Veen, A. H. Zewail, ACS Nano 2015, 9, 1721.
[25] R. Senga, K. Suenaga, Ultramicroscopy 2017, 180, 150.
[26] M. Haider, H. Rose, S. Uhlemann, E. Schwan, B. Kabius, K. Urban, Ultramicroscopy 1998, 75, 53; K. W. Urban, Science 2008, 321, 506.
[27] J. H. Warner, N. P. Young, A. I. Kirkland, G. A. D. Briggs, Nat Mater 2011, 10, 958.
[28] K. Suenaga, H. Wakabayashi, M. Koshino, Y. Sato, K. Urita, S. Iijima, Nat Nano 2007, 2, 358.
[29] L.-C. Qin, Rep Prog Phys 2006, 69, 2761.
[30] R. Senga, H.-P. Komsa, Z. Liu, K. Hirose-Takai, A. V. Krasheninnikov, K. Suenaga, Nat Mater 2014, 13, 1050.
[31] K. Suenaga, M. Koshino, Nature 2010, 468, 1088.
[32] R. Senga, T. Pichler, K. Suenaga, Nano Lett 2016, 16, 3661.

[33] R. Senga, K. Suenaga, P. Barone, S. Morishita, F. Mauri, T. Pichler, Nature 2019, 573, 247; R. Senga, Y.-C. Lin, S. Morishita, R. Kato, T. Yamada, M. Hasegawa, K. Suenaga, Nature 2022, 603, 68.

[34] O. Cretu, D.-M. Tang, D.-B. Lu, B. Da, Y. Nemoto, N. Kawamoto, M. Mitome, Z. Ding, K. Kimoto, Carbon 2023, 201, 1025.

[35] Y. Jiang, Z. Chen, Y. Han, P. Deb, H. Gao, S. Xie, P. Purohit, M. W. Tate, J. Park, S. M. Gruner, V. Elser, D. A. Muller, Nature 2018, 559, 343; Z. Chen, Y. Jiang, Y.-T. Shao, M. E. Holtz, M. Odstrčil, M. Guizar-Sicairos, I. Hanke, S. Ganschow, D. G. Schlom, D. A. Muller, Science 2021, 372, 826.

[36] P. M. Pelz, S. M. Griffin, S. Stonemeyer, D. Popple, H. DeVyldere, P. Ercius, A. Zettl, M. C. Scott, C. Ophus, Nat Commun 2023, 14, 7906.

[37] Y. Wang, L. Qiu, L. Zhang, D.-M. Tang, R. Ma, Y. Wang, B. Zhang, F. Ding, C. Liu, H.-M. Cheng, ACS Nano 2020, 14, 16823.

[38] D.-M. Tang, C. Liu, W.-J. Yu, L.-L. Zhang, P.-X. Hou, J.-C. Li, F. Li, Y. Bando, D. Golberg, H.-M. Cheng, ACS Nano 2014, 8, 292.

[39] D. Golberg, P. M. F. J. Costa, M.-S. Wang, X. Wei, D.-M. Tang, Z. Xu, Y. Huang, U. K. Gautam, B. Liu, H. Zeng, N. Kawamoto, C. Zhi, M. Mitome, Y. Bando, Adv Mater 2012, 24, 177; D. S. Su, B. Zhang, R. Schlögl, Chem Rev 2015, 115, 2818; D.-M. Tang, O. Cretu, S. Ishihara, Y. Zheng, K. Otsuka, R. Xiang, S. Maruyama, H.-M. Cheng, C. Liu, D. Golberg, Nature Reviews Electrical Engineering 2024, 1, 149.

[40] E. D. Boyes, P. L. Gai, Ultramicroscopy 1997, 67, 219; R. Sharma, K. Weiss, Microsc Res Techniq 1998, 42, 270; J. B. Wagner, F. Cavalca, C. D. Damsgaard, L. D. L. Duchstein, T. W. Hansen, Micron 2012, 43, 1169; S. Takeda, Y. Kuwauchi, H. Yoshida, Ultramicroscopy 2015, 151, 178.

[41] R. T. K. Baker, M. A. Barber, P. S. Harris, F. S. Feates, R. J. Waite, J Catal 1972, 26, 51.

[42] S. Helveg, C. López-Cartes, J. Sehested, P. L. Hansen, B. S. Clausen, J. R. Rostrup-Nielsen, F. Abild-Pedersen, J. K. Nørskov, Nature 2004, 427, 426; R. Sharma, Z. Iqbal, Appl Phys Lett 2004, 84, 990.

[43] S. Hofmann, R. Sharma, C. Ducati, G. Du, C. Mattevi, C. Cepek, M. Cantoro, S. Pisana, A. Parvez, F. Cervantes-Sodi, A. C. Ferrari, R. Dunin-Borkowski, S. Lizzit, L. Petaccia, A. Goldoni, J. Robertson, Nano Lett 2007, 7, 602.

[44] H. Yoshida, S. Takeda, T. Uchiyama, H. Kohno, Y. Homma, Nano Lett 2008, 8, 2082.

[45] S. Hofmann, R. Blume, C. T. Wirth, M. Cantoro, R. Sharma, C. Ducati, M. Havecker, S. Zafeiratos, P. Schnoerch, A. Oestereich, D. Teschner, M. Albrecht, A. Knop-Gericke, R. Schlögl, J. Robertson, J Phys Chem C 2009, 113, 1648; C. T. Wirth, S. Hofmann, J. Robertson, Diam Relat Mater 2009, 18, 940.

[46] C. T. Wirth, B. C. Bayer, A. D. Gamalski, S. Esconjauregui, R. S. Weatherup, C. Ducati, C. Baehtz, J. Robertson, S. Hofmann, Chem Mater 2012, 24, 4633.
[47] P. A. Lin, J. L. Gomez-Ballesteros, J. C. Burgos, P. B. Balbuena, B. Natarajan, R. Sharma, J Catal 2017, 349, 149.
[48] R. Sharma, Micron 2012, 43, 1147.
[49] L. F. Allard, S. H. Overbury, W. C. Bigelow, M. B. Katz, D. P. Nackashi, J. Damiano, Microsc Microanal 2012, 18, 656.
[50] J. Yang, O. Paul, Sensors and Actuators A: Physical 2002, 97-98, 520.
[51] T. Yokosawa, T. Alan, G. Pandraud, B. Dam, H. Zandbergen, Ultramicroscopy 2012, 112, 47.
[52] N. de Jonge, W. C. Bigelow, G. M. Veith, Nano Lett 2010, 10, 1028.
[53] H. H. Pérez Garza, D. Morsink, J. Xu, M. Sholkina, Y. Pivak, M. Pen, S. van Weperen, Q. Xu, Micro & Nano Letters 2017, 12, 69.
[54] X. Huang, R. Farra, R. Schlögl, M.-G. Willinger, Nano Lett 2019, 19, 5380.
[55] Y. Lyu, P. Wang, D. Liu, F. Zhang, T. P. Senftle, G. Zhang, Z. Zhang, J. Wang, W. Liu, Small Methods 2022, 6, 2200235.
[56] M. Bahri, K. Dembélé, C. Sassoye, D. P. Debecker, S. Moldovan, A. S. Gay, C. Hirlimann, C. Sanchez, O. Ersen, Nanoscale 2018, 10, 14957.
[57] H. Fan, L. Qiu, A. Fedorov, M.-G. Willinger, F. Ding, X. Huang, ACS Nano 2021, 15, 17895.
[58] Y. Wang, L. Qiu, L. Zhang, D.-M. Tang, R. Ma, C.-L. Ren, F. Ding, C. Liu, H.-M. Cheng, Sci Adv 2022, 8, eabo5686.
[59] F. Banhart, Small 2024, n/a, 2310462.
[60] B. Liu, D.-M. Tang, C. Sun, C. Liu, W. Ren, F. Li, W.-J. Yu, L.-C. Yin, L. Zhang, C. Jiang, H.-M. Cheng, J Am Chem Soc 2011, 133, 197.
[61] K. Cao, T. W. Chamberlain, J. Biskupek, T. Zoberbier, U. Kaiser, A. N. Khlobystov, Nano. Lett. 2018, 18, 6334.
[62] Y. Hu, L. Zhu, Y. Peng, J. Fu, X. Deng, J. Zhang, H. Zhang, C. Guan, A. Karim, X. Zhang, ChemCatChem 2020, 12, 1316.
[63] A. Chuvilin, A. N. Khlobystov, D. Obergfell, M. Haluska, S. Yang, S. Roth, U. Kaiser, Angew Chem Int Edit 2010, 49, 193.
[64] T. Zoberbier, T. W. Chamberlain, J. Biskupek, N. Kuganathan, S. Eyhusen, E. Bichoutskaia, U. Kaiser, A. N. Khlobystov, J Am Chem Soc 2012, 134, 3073.
[65] H. L. Xin, K. Niu, D. H. Alsem, H. Zheng, Microsc Microanal 2013, 19, 1558.
[66] K. Koo, S. M. Ribet, C. Zhang, P. J. M. Smeets, R. dos Reis, X. Hu, V. P. Dravid, Nano Lett 2022, 22, 4137.
[67] F. Yang, M. Wang, D. Zhang, J. Yang, M. Zheng, Y. Li, Chem Rev 2020, 120, 2693.
[68] H.-a. Mehedi, J. Ravaux, S. Tahir, R. Podor, V. Jourdain, *In situ study of single-*

walled carbon nanotube growth in an environmental scanning electron microscope, Vol. 27, 2016.

[69] H.-Y. Chao, H. Jiang, J. Cumings, R. Sharma, Microsc Microanal 2019, 25, 1452.

[70] H.-Y. Chao, H. Jiang, F. Ospina-Acevedo, P. B. Balbuena, E. I. Kauppinen, J. Cumings, R. Sharma, Nanoscale 2020, 12, 21923.

[71] S. Mazzucco, Y. Wang, M. Tanase, M. Picher, K. Li, Z. Wu, S. Irle, R. Sharma, J Catal 2014, 319, 54.

[72] Z. Hussaini, P. A. Lin, B. Natarajan, W. Zhu, R. Sharma, Ultramicroscopy 2018, 186, 139.

[73] S. Helveg, C. Lopez-Cartes, J. Sehested, P. L. Hansen, B. S. Clausen, J. R. Rostrup-Nielsen, F. Abild-Pedersen, J. K. Norskov, Nature 2004, 427, 426.

[74] R. Rao, R. Sharma, F. Abild-Pedersen, J. K. Norskov, A. R. Harutyunyan, Sci. Rep. 2014, 4.

[75] Y. Lyu, P. Wang, D. Liu, F. Zhang, T. P. Senftle, G. Zhang, Z. Zhang, J. Wang, W. Liu, Small Methods 2022, 6, e2200235.

[76] R.-H. Xie, L. Zhang, R. Ma, X.-Y. Jiao, D.-M. Tang, C. Liu, H.-M. Cheng, Nano Res 2023, 16, 12781.

[77] F. Yang, H. Zhao, X. Wang, X. Liu, Q. Liu, X. Liu, C. Jin, R. Wang, Y. Li, J Am Chem Soc 2019, 141, 5871.

[78] H. An, A. Kumamoto, R. Xiang, T. Inoue, K. Otsuka, S. Chiashi, C. Bichara, A. Loiseau, Y. Li, Y. Ikuhara, S. Maruyama, Sci Adv 2019, 5, eaat9459.

[79] W. H. Chiang, R. M. Sankaran, Nat Mater 2009, 8, 882.

[80] A. R. Harutyunyan, G. G. Chen, T. M. Paronyan, E. M. Pigos, O. A. Kuznetsov, K. Hewaparakrama, S. M. Kim, D. Zakharov, E. A. Stach, G. U. Sumanasekera, Science 2009, 326, 116.

[81] R. Ma, L. Qiu, L. Zhang, D.-M. Tang, Y. Wang, B. Zhang, F. Ding, C. Liu, H.-M. Cheng, ACS Nano 2022, 16, 16574.

[82] R. S. Wagner, W. C. Ellis, Appl Phys Lett 1964, 4, 89.

[83] B. Liu, D. M. Tang, C. Sun, C. Liu, W. Ren, F. Li, W. J. Yu, L. C. Yin, L. Zhang, C. Jiang, H. M. Cheng, J Am Chem Soc 2010, 133, 197.

[84] T. Maruyama, in *Handbook of Carbon Nanotubes*, (Eds: J. Abraham, S. Thomas, N. Kalarikkal), Springer International Publishing, Cham 2022, 57.

[85] F. Yang, H. Zhao, W. Wang, Q. Liu, X. Liu, Y. Hu, X. Zhang, S. Zhu, D. He, Y. Xu, J. He, R. Wang, Y. Li, CCS Chemistry 2020, 0.

[86] F. Yang, H. Zhao, R. Li, Q. Liu, X. Zhang, X. Bai, R. Wang, Y. Li, Sci Adv 2022, 8, eabq0794.

[87] M. C. Diaz, H. Jiang, E. Kauppinen, R. Sharma, P. B. Balbuena, The Journal of Physical Chemistry C 2019, 123, 30305.

[88] R. Rao, N. Pierce, D. Liptak, D. Hooper, G. Sargent, S. L. Semiatin, S. Curtarolo, A. R. Harutyunyan, B. Maruyama, ACS Nano 2013, 7, 1100; R. Rao, A. E. Islam, N. Pierce, P. Nikolaev, B. Maruyama, Carbon 2015, 95, 287; H. Navas, M. Picher, A. Andrieux-Ledier, F. Fossard, T. Michel, A. Kozawa, T. Maruyama, E. Anglaret, A. Loiseau, V. Jourdain, ACS Nano 2017, 11, 3081.

[89] S. Jeong, J. Lee, H.-C. Kim, J. Y. Hwang, B.-C. Ku, D. N. Zakharov, B. Maruyama, E. A. Stach, S. M. Kim, Nanoscale 2016.

[90] M. F. C. Fiawoo, A. M. Bonnot, H. Amara, C. Bichara, J. Thibault-Pénisson, A. Loiseau, Phys Rev Lett 2012, 108, 195503.

[91] H. Zhu, K. Suenaga, J. Wei, K. Wang, D. Wu, J Cryst Growth 2008, 310, 5473.

[92] H. Zhu, K. Suenaga, A. Hashimoto, K. Urita, K. Hata, S. Iijima, Small 2005, 1, 1180.

[93] D.-M. Tang, L.-L. Zhang, C. Liu, L.-C. Yin, P.-X. Hou, H. Jiang, Z. Zhu, F. Li, B. Liu, E. I. Kauppinen, H.-M. Cheng, Scientific Reports 2012, 2, 971.

[94] J. L. Maurice, D. Pribat, Z. He, G. Patriarche, C. S. Cojocaru, Carbon 2014, 79, 93.

[95] L. Qiu, F. Ding, Small 2022, n/a, 2204437.

[96] X. Zhang, D. Tian, F. Yang, H. Zhao, W.-M. Lau, R. Wang, Advanced Materials Interfaces 2022, n/a, 2200334.

[97] M. He, X. Wang, S. Zhang, H. Jiang, F. Cavalca, H. Cui, J. B. Wagner, T. W. Hansen, E. Kauppinen, J. Zhang, F. Ding, Sci. Adv. 2019, 5, eaav9668; M. He, H. Jiang, I. Kauppi, P. V. Fedotov, A. I. Chernov, E. D. Obraztsova, F. Cavalca, J. B. Wagner, T. Hansen, J. Sainio, E. sairanen, J. Lehtonen, E. Kauppinen, J Mater Chem A 2014, 2, 5883.

[98] M. He, H. Jiang, B. Liu, P. V. Fedotov, A. I. Chernov, E. D. Obraztsova, F. Cavalca, J. B. Wagner, T. W. Hansen, I. V. Anoshkin, E. A. Obraztsova, A. V. Belkin, E. Sairanen, A. G. Nasibulin, J. Lehtonen, E. I. Kauppinen, Sci Rep 2013, 3.

[99] M. Picher, P. A. Lin, J. L. Gomez-Ballesteros, P. B. Balbuena, R. Sharma, Nano Lett 2014, 14, 6104.

[100] E. L. Lawrence, P. A. Crozier, ACS Applied Nano Materials 2018, 1, 1360.

[101] Q. Wu, L. Qiu, L. Zhang, H. Liu, R. Ma, P. Xie, R. Liu, P. Hou, F. Ding, C. Liu, M. He, Chem Eng J 2021, 431, 133487.

[102] F. Yang, H. Zhao, W. Wang, L. Wang, L. Zhang, T. Liu, J. Sheng, S. Zhu, D. He, L. Lin, J. He, R. Wang, Y. Li, Chemical Science 2021, 12, 12651.

[103] M. Bedewy, B. Viswanath, E. R. Meshot, D. N. Zakharov, E. A. Stach, A. J. Hart, Chem Mater 2016, 28, 3804.

[104] P. A. Lin, J. L. Gomez-Ballesteros, J. C. Burgos, P. B. Balbuena, B. Natarajan, R. Sharma, J Catal 2017, 349, 149.

[105] Z. Hussaini, P. A. Lin, W. Zhu, B. Natarajan, R. Sharma, Microsc Microanal 2016, 22, 718.

[106] J. Zhao, A. Martinez-Limia, P. B. Balbuena, Nanotechnology 2005, 16, S575.
[107] M. S. He, X. Wang, S. C. Zhang, H. Jiang, F. Cavalca, H. Z. Cui, J. B. Wagner, T. W. Hansen, E. Kauppinen, J. Zhang, F. Ding, Sci Adv 2019, 5.
[108] R. Sharma, P. Rez, M. Brown, G. H. Du, M. M. J. Treacy, Nanotechnology 2007, 18.
[109] K. Dembélé, M. Bahri, G. Melinte, C. Hirlimann, A. Berliet, S. Maury, A.-S. Gay, O. Ersen, ChemCatChem 2018, 10, 4004.
[110] A. Gamalski, E. S. Moore, M. M. J. Treacy, R. Sharma, P. Rez, Appl Phys Lett 2009, 95, 233109.
[111] R. Sharma, P. Rez, M. M. J. Treacy, S. J. Stuart, J Electron Microsc 2005, 54, 231.
[112] F. Ding, A. R. Harutyunyan, B. I. Yakobson, Proc Natl Acad Sci USA 2009, 106, 2506.
[113] J. A. Rodríguez-Manzo, M. Terrones, H. Terrones, H. W. Kroto, L. Sun, F. Banhart, Nat. Nanotechnol. 2007, 2, 307.
[114] D. M. Tang, C. Liu, W. J. Yu, L. Zhang, P. X. Hou, J. C. Li, F. Li, Y. Bando, D. Golberg, H. M. Cheng, ACS Nano 2013, 8, 292.
[115] H. Dai, A. G. Rinzler, P. Nikolaev, A. Thess, D. T. Colbert, R. E. Smalley, Chem Phys Lett 1996, 260, 471.
[116] E. Pigos, E. S. Penev, M. A. Ribas, R. Sharma, B. I. Yakobson, A. R. Harutyunyan, ACS Nano 2011, 5, 10096.
[117] L. Zhang, Z. Xu, T.-l. Feng, M. He, T. W. Hansen, J. B. Wagner, C. Liu, H.-M. Cheng, Advanced Science 2023, 10, 2304905.
[118] L. L. Zhang, P. X. Hou, S. S. Li, C. Shi, H. T. Gong, C. Liu, H. M. Cheng, J Phys Chem Lett. 2014, 5, 1427.
[119] L. Zhang, M. He, T. W. Hansen, J. Kling, H. Jiang, E. I. Kauppinen, A. Loiseau, J. B. Wagner, ACS Nano 2017, 11, 4483.
[120] S. Ahmad, Q. Zhang, E.-X. Ding, H. Jiang, E. I. Kauppinen, Chem Phys Lett 2023, 810, 140185.
[121] R. Sharma, Z. Iqbal, Appl Phys Lett 2004, 84, 990.
[122] M. Lin, J. P. Y. Tan, C. Boothroyd, K. P. Loh, E. S. Tok, Y. L. Foo, Nano Lett 2006, 6, 449.
[123] R. Sharma, Microsc Res Techniq 2009, 72, 144.
[124] T. A. J. Welling, S. E. Schoemaker, K. P. de Jong, P. E. de Jongh, J. Phys. Chem. C. 2023, 127, 15766.
[125] L. Zhang, Z. Xu, T.-l. Feng, M. He, T. W. Hansen, J. B. Wagner, C. Liu, H.-M. Cheng, Advanced Science 2023, 2304905.
[126] Y. Kohigashi, H. Yoshida, Y. Homma, S. Takeda, Appl Phys Lett 2014, 105.
[127] H. Yoshida, S. Takeda, Carbon 2014, 70, 266.
[128] V. Balakrishnan, M. Bedewy, E. R. Meshot, S. W. Pattinson, E. S. Polsen, F. Laye,

D. N. Zakharov, E. A. Stach, A. J. Hart, ACS Nano 2016, 10, 11496.
[129] S. Maruyama, E. Einarsson, Y. Murakami, T. Edamura, Chem Phys Lett 2005, 403, 320.
[130] M. Stadermann, S. P. Sherlock, J. B. In, F. Fornasiero, H. G. Park, A. B. Artyukhin, Y. M. Wang, J. J. De Yoreo, C. P. Grigoropoulos, O. Bakajin, A. A. Chernov, A. Noy, Nano Lett 2009, 9, 738.
[131] P. B. Amama, C. L. Pint, L. McJilton, S. M. Kim, E. A. Stach, P. T. Murray, R. H. Hauge, B. Maruyama, Nano Lett 2008, 9, 44.
[132] S. M. Kim, C. L. Pint, P. B. Amama, D. N. Zakharov, R. H. Hauge, B. Maruyama, E. A. Stach, J Phys Chem Lett. 2010, 1, 918.
[133] M. Picher, E. Anglaret, R. Arenal, V. Jourdain, Nano Lett 2009, 9, 542.
[134] F. Ding, P. Larsson, J. A. Larsson, R. Ahuja, H. Duan, A. Rosén, K. Bolton, Nano Lett 2007, 8, 463.
[135] G. Zhaoli, M. M. F. Yuen, "Study of CNT growth termination mechanism: Effect of catalyst diffusion", presented at *Thermal, Mechanical and Multi-Physics Simulation and Experiments in Microelectronics and Microsystems (EuroSimE), 2012 13th International Conference on*, 16-18 April 2012, 2012.
[136] S. M. Kim, C. L. Pint, P. B. Amama, R. H. Hauge, B. Maruyama, E. A. Stach, J Mater Res 2011, 25, 1875.
[137] D. Yi, D. Luo, Z. J. Wang, J. Dong, X. Zhang, M. G. Willinger, R. S. Ruoff, F. Ding, Phys Rev Lett 2018, 120, 246101.
[138] W. Cho, M. Schulz, V. Shanov, Carbon 2014, 69, 609.

Lili Zhang is a professor at the Institute of Metal Research (IMR), Chinese Academy of Sciences (CAS). She received her Ph.D. in materials science at IMR, CAS in 2014 and then worked as a postdoc at Technical University of Denmark in Denmark till 2017. Her main research interests are controlled growth of carbon nanotubes by CVD, their growth mechanisms and structure-property relationships by means of *in situ* TEM

especially ETEM.

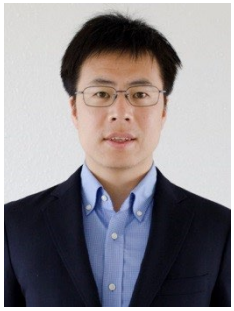

Dai-Ming Tang is a Principal Researcher at Research Center for Materials Nanoarchitectonics (MANA), National Institute for Materials Science (NIMS) and an Associate Professor at Institute of Pure and Applied Sciences, University of Tsukuba (Collaborative University). He received his B.Sc. in materials science and engineering in Xiangtan University, China in 2004, and his Ph.D. in materials science from Institute of Metal Research, Chinese Academy of Sciences, China, in 2010. His research interests include growth mechanism, fundamental properties, electronic and quantum devices of CNTs and CNT molecular junctions.

Chang Liu is a professor of the Institute of Metal Research (IMR), Chinese Academy of Sciences (CAS). He received his Ph.D. in materials science at IMR, CAS in 2000. He mainly works on the preparation and application of carbon nanotubes and their hybrids.